

Stony Brook University



OFFICIAL COPY

The official electronic file of this thesis or dissertation is maintained by the University Libraries on behalf of The Graduate School at Stony Brook University.

© All Rights Reserved by Author.

Synthesis of Tetrahedral Chromophore Arrays for Applications in FRET Studies

A Thesis Presented

by

Sarah Jeanine Richards

to

The Graduate School

in Partial Fulfillment of the

Requirements

for the Degree of

Master of Science

in

Chemistry

Stony Brook
University

August 2007

STONY BROOK
UNIVERSITY

The Graduate School

Sarah Jeanine Richards

We, the thesis committee for the above candidate for the
Master of Science degree, hereby recommend
acceptance of this thesis.

Dr. Nancy S. Goroff, Advisor
Department of Chemistry

Dr. Kathlyn A. Parker, Chairperson
Department of Chemistry

Dr. Isaac Carrico, Third Member
Department of Chemistry

This thesis is accepted by the Graduate School

Lawrence Martin
Dean of the Graduate School

Abstract of the Thesis

**Synthesis of Tetrahedral Chromophore Arrays
for Applications in FRET Studies**

by

Sarah Jeanine Richards

Master of Science

in

Chemistry

Stony Brook
University

2007

Förster Resonance Energy Transfer (FRET) has become a useful technique to study the structures and dynamics of biological molecules and systems. However, FRET is limited by the orientation of the chromophores at the time of energy transfer. Therefore, accurate distances can only be established for systems where the chromophores are able to rotate freely on a flexible tether. The angular dependence would be reduced or eliminated through the use of isotropic three-dimensional chromophores. Described in this thesis are efforts toward the design and synthesis of tetrahedral arrays of fluorescein and Tokyo Green chromophores, attached to a tetraaryl silane core (shown in Figure 1). We have developed a synthetic route that focuses on coupling the xanthene unit of the chromophore with a tetraaryl moiety using a Grignard reaction. We have prepared the tetraaryl

core, tetrakis (4-bromo-2-methylphenyl) silane, and protected xanthenes, including bis-TBS xanthone and bis-MEM xanthone. We also report efforts to couple the xanthone and aryl moieties and a successful model coupling to prepare the chromophore Tokyo Green.

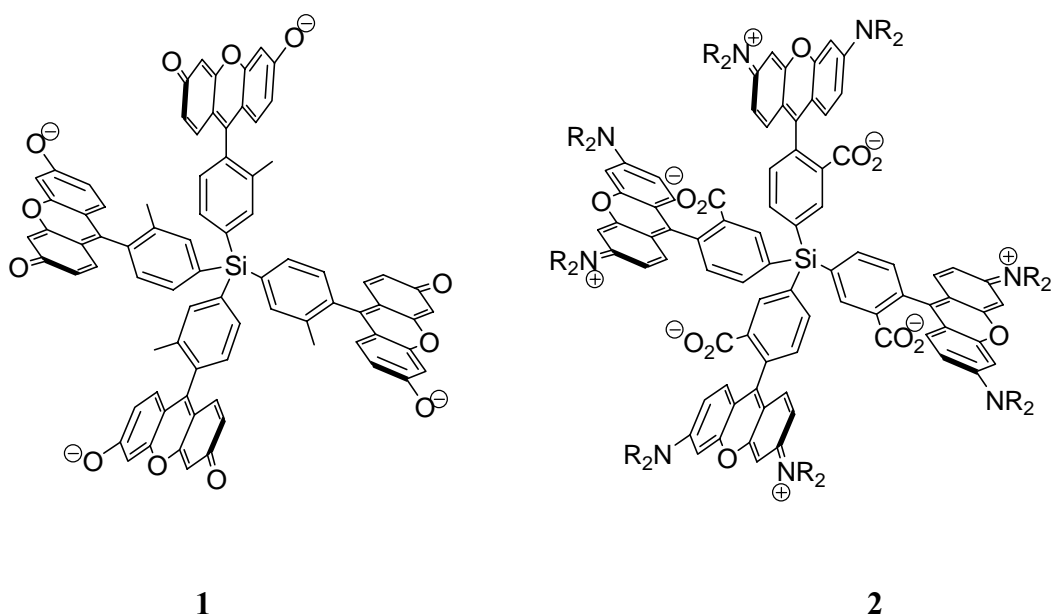


Figure 1. Two target molecules: tetrahedral assemblies of Tokyo Green (1) and rhodamine B (2).

Table of Contents

| | |
|---|------|
| List of Schemes | vi |
| List of Figures | vii |
| List of Abbreviations | viii |
| I. Introduction | 1 |
| II. Project Design | 10 |
| III. Synthesis | 18 |
| a. Strategy 1 | 18 |
| b. Strategy 2 | 20 |
| c. Strategy 3 | 24 |
| i. Synthesis of xanthene moiety | 26 |
| ii. Synthesis of tetraaryl silane core | 30 |
| iii. Model reactions for coupling of xanthone to core | 30 |
| iv. Successful coupling to make Tokyo Green | 39 |
| v. Proposed new tetraaryl silane core | 41 |
| IV. Future Work | 45 |
| V. Experimental | 46 |
| VI. References | 61 |
| VII. Appendix | 65 |

List of Schemes

| | | |
|-------------------|---|----|
| Scheme 1: | Proposed synthesis for building the chromophores up on the silane core. | 19 |
| Scheme 2: | Proposed synthesis for preparing the chromophores and then attaching them to the silane core. | 22 |
| Scheme 3: | Proposed method for preparing the xanthene and aryl moieties and then attaching them through Grignard coupling. | 26 |
| Scheme 4: | Reaction to synthesize 3,6-Bis-(2-methoxyethoxymethoxy)xanthen-9-one 17 . | 29 |
| Scheme 5: | Model Reaction 1 using Urano method. | 31 |
| Scheme 6: | Model Reaction 2 using n-BuLi and MgBr ₂ . | 32 |
| Scheme 7: | Model Reaction 3 to synthesize Tokyo Green. | 34 |
| Scheme 8: | Proposed reaction to synthesize array 1 using Peterson procedure. | 35 |
| Scheme 9: | Model reaction 4 to prepare Tokyo Green. | 36 |
| Scheme 10: | Model reaction 5 to prepare Tokyo Green. | 38 |
| Scheme 11: | Synthesis of tetrakis(4-iodo-2-methylphenyl)silane 24 . | 42 |
| Scheme 12: | Proposed model reaction and reaction to target array 1 . | 44 |

List of Figures

| | | |
|-------------------|---|----|
| Figure 1: | Two target molecules: tetrahedral assemblies of Tokyo Green (1) and rhodamine B (2). | iv |
| Figure 2: | Schematic of the FRET mechanism when a donor and acceptor's interchromophore distance is less than 10 Å. | 3 |
| Figure 3: | Illustration showing the exponential relationship of distance, R, to the efficiency of energy transfer, E. | 6 |
| Figure 4: | A schematic representation of the donor and acceptor absorption and emission spectra for application as a FRET pair. | 7 |
| Figure 5: | The relative orientation of the donor (θ_D) and acceptor (θ_A) transition dipoles. | 9 |
| Figure 6: | Examples of organic dyes from the xanthene family. | 12 |
| Figure 7: | Goodson and coworkers found that intra-array FRET occurs on a sub-picosecond timescale. | 14 |
| Figure 8: | Tokyo Green structure divided into its two parts, the xanthene and benzene moieties. | 15 |
| Figure 9: | The three degenerate HOMO's, each localized on one of the chromophores, for a pseudotetrahedral array of three rhodamines on a silane core (PM3 calculation). | 17 |
| Figure 10: | The three degenerate LUMO's, each localized on one of the chromophores, for a pseudotetrahedral array of three rhodamines on a silane core (PM3 calculation). | 17 |
| Figure 11: | The two principle isomers of rhodamine B and charged states that are possible. | 20 |

| | | |
|-------------------|---|----|
| Figure 12: | Effects on fluorescence properties due to substitution on benzene moiety. | 24 |
| Figure 13: | Crystal structure of tetrakis(4-bromo-2-methylphenyl)-silane 14 . | 30 |

List of Abbreviations

Å: Angstrom unit

Ac: Acetyl

AFM: atomic force microscopy

n-BuLi: n-Butyl lithium

°C: degrees Celsius

d: doublet

DMF: dimethylformamide

DMSO: dimethylsulfoxide

E: FRET efficiency

Ex and Em: excitation wavelength and emission wavelength

eV: electron volts

f_D : normalized donor emission spectrum

FRET: Förster resonance energy transfer

fs: femtoseconds

h: hour

HCl: hydrochloric acid

HOMO: highest occupied molecular orbital

I_D : fluorescence intensity of donor in absence of acceptor

I_{DA} : fluorescence intensity of donor in presence of acceptor

i-PrMgCl: isopropyl- magnesium chloride

J_{da} : Spectral overlap of donor emission and the acceptor's absorption

κ^2 : angular orientation factor

LUMO: lowest unoccupied molecular orbital

m: multiplet

MEM: methoxyethoxymethyl

MeOH: methanol

MHz: megahertz

min: minutes

mL: mililiter

MOM: methoxymethyl

MS: mass spectrometry

mmol: millimoles

n : refractive index of the medium

nm: nanometer

NMR: nuclear magnetic resonance

NSOM: near-field scanning optical microscopy

PeT: photoinduced electron transfer

Ph: phenyl

PMA: phosphomolybdic acid in ethanol

PM3: parameterized model number 3

ppm: parts per million

q: quartet

R: distance between donor and acceptor chromophores

RBF: round-bottom flask

R_0 : Förster radius

rt: room temperature

s: singlet

t: triplet

T_D : fluorescence lifetime of donor in absence of acceptor

T_{DA} : fluorescence lifetime of donor in presence of acceptor

TFA: trifluoroacetic acid

TBS: *t*-butyldimethylsilyl

THF: tetrahydrofuran

TIPS: triisopropylsilyl

TLC: thin layer chromatography

TMS: trimethylsilyl

UV: ultraviolet

Φ : angle between the two planes with the transition dipoles of the chromophore pair

Φ_D : fluorescence quantum yield of the donor

ϵ_A : acceptor extinction coefficient

λ : wavelength

θ_D : relative orientation of the donor transition dipole

θ_A : relative orientation of the acceptor transition dipole

I. Introduction

Förster Resonance Energy Transfer (FRET) has been used in various areas from biophysics to polymer science.¹⁻³ It has applications in many biological investigations, not only as a measurement of distance on a macromolecule, but to study protein-protein interactions, protein conformational changes, and complex formation between a ligand and receptor. FRET has also been used to increase the resolution of atomic force microscopy (AFM) imaging techniques and in confocal laser scanning microscopy and flow cytometry.³⁵ FRET can be used to characterize distance-dependent interactions on a nanometer scale, in a range of approximately 20 to 100 Å. FRET spectroscopy is one of the few tools that can measure intermolecular and intramolecular energy transfers both *in vivo* and *in vitro*.¹

The first discovery that led to the development of FRET was in the early 1930's by Jean-Baptiste Perrin. Perrin recognized that a fluorochrome in its excited state behaves like an oscillating dipole that creates its own characteristic

electric field. If an acceptor enters the donor field, energy can transfer from the donor by direct electrodynamic interactions and induce transitions in the acceptor, with no intermediate photon involved. But it was German scientist Theodor Förster who developed the quantum-mechanical basis and the equations that are used to understand FRET studies today.^{1,5} He found that the efficiency of energy transfer will vary as the inverse of the sixth power of the distance separating the donor and acceptor, and defined the critical molecular separation distance, R_0 , known as the Förster radius.

The FRET mechanism occurs between two fluorescent groups (Figure 2). One chromophore, the donor, absorbs light at a certain wavelength, to form an excited state. This excitation is then non-radiatively transferred, by long-range dipole-dipole interactions, to a second chromophore, the acceptor, quenching the donor fluorescence and reducing the donor's fluorescence lifetime. The acceptor molecule then emits light at a longer wavelength. Since FRET is not mediated by photon emission from the donor, it does not require the acceptor to be fluorescent and it is not the result of a collision with the acceptor. If both chromophores are fluorescent it is sometimes referred to as Fluorescence Resonance Energy Transfer.

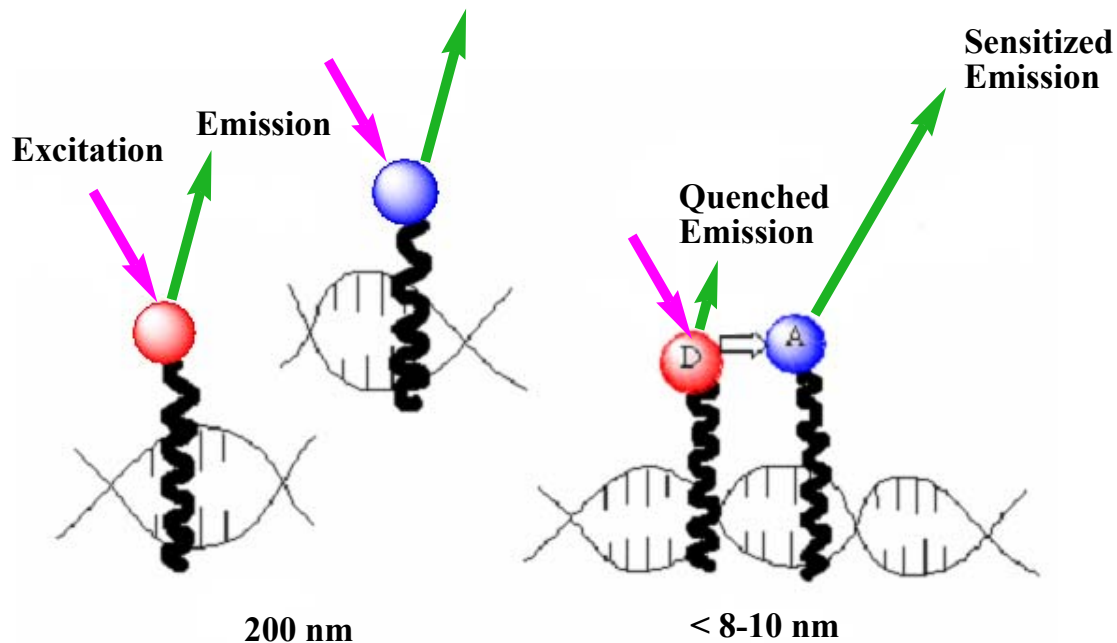


Figure 2. Schematic of the FRET mechanism when a donor and acceptor's interchromophore distance is less than 10 Å.

The Förster equation shows that the efficiency of energy transfer (E) is highly dependent on the distance between the two chromophores (R). The FRET efficiency (E), which is the fraction of energy absorbed by the donor that is subsequently transferred to the acceptor, can be obtained by measuring the fluorescence intensities of the donor in the presence (I_{DA}) and absence (I_D) of the acceptor (Equation 1).

$$(1) \quad E = 1 - (I_{DA} / I_D)$$

FRET efficiency can also be measured using the lifetime of the donor in the presence (T_{DA}) and absence (T_D) of the acceptor (Equation 2).

$$(2) \quad E = 1 - (T_{DA} / T_D)$$

The relationship between the efficiency of energy transfer (E) and the distance between the chromophores (R) is given is Equation 3.¹

$$(3) \quad E = R_0^6 / (R^6 + R_0^6)$$

The Förster radius (R_0), or Förster critical distance, which can be calculated by Equation 4, is defined as the distance where 1/2 of the energy is transferred. Its value is a function of the angular orientation factor (κ^2), refractive index of the medium (n), the fluorescence quantum yield of the donor (Φ_d), and the spectral overlap integral between the donor and the acceptor (J_{da}).^{1,2}

$$(4) \quad R_0^6 = (8.79 \times 10^{23}) \kappa^2 n^{-4} \Phi_d J_{da}$$

The refractive index of the medium is usually known from the solvent, or can be estimated for certain molecules. It is generally assumed to be 1.4 for proteins and aqueous solutions, but can range from 1.33 to 1.6. The quantum yield of the donor in absence of the acceptor is the ratio of the amount of light emitted from the sample to the amount of light absorbed by the sample. This is determined by comparing to standard fluorophores with known quantum yields.¹

The FRET efficiency is determined by three main parameters according to the above equations; the distance between the donor and acceptor chromophore, the spectral overlap between the donor emission and the acceptor absorption, and the relative angular orientation in space between the transition dipole of the donor and acceptor.

Since the efficiency of energy transfer falls off by a factor of R^6 , FRET is a particularly sensitive measurement of distance. But, also due to this dependence, R can only be measured accurately when this donor-acceptor distance is close to the Förster radius, $0.5R_0$ to $1.5R_0$. Figure 3 shows the exponential relationship between transfer efficiency and the distance separating the donor and acceptor. When R is 50% of R_0 the energy transfer is near maximum and shorter distances can not be reliably determined. When it is over by 50%, efficiency is near zero, so that longer distances can not be measured.³⁵ The typical R_0 range for FRET measurements is roughly 20 to 60 Å, depending on the choice of donor and acceptor chromophores, therefore distances can be measured by FRET over a range of 10 to 80 Å.³

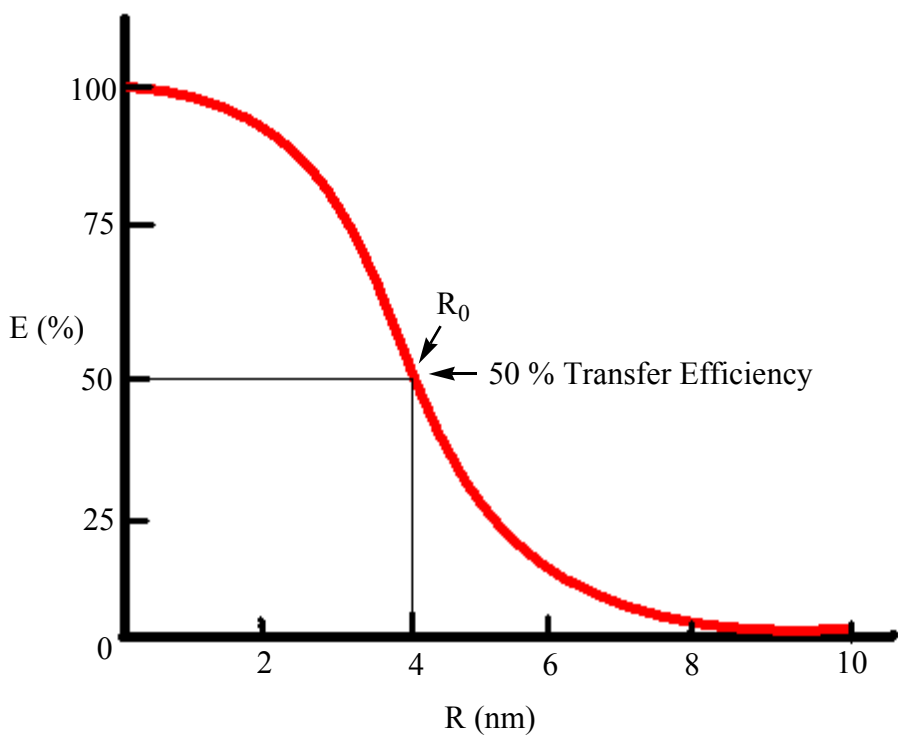


Figure 3. Illustration showing the exponential relationship of distance, R, to the efficiency of energy transfer, E.

The second parameter that determines FRET efficiency is the degree of donor/acceptor spectral overlap. The donor emission spectrum must overlap the absorption spectrum of the acceptor, as seen in Figure 4. As long as there is partial overlap, resonance energy transfer can occur. The extent of spectral overlap will influence the rate of energy transfer. The more the spectra overlap, the stronger the FRET efficiency, but if the spectral overlap is increased too much, “spectral bleed-through” or “crossover” can occur, resulting in high

background noise. Acceptor bleed-through refers to direct photo excitation of the acceptor. It can occur when the acceptor absorbs at the wavelengths used to excite the donor. Donor crosstalk refers to donor emission detected in the acceptor emission channel.³⁵

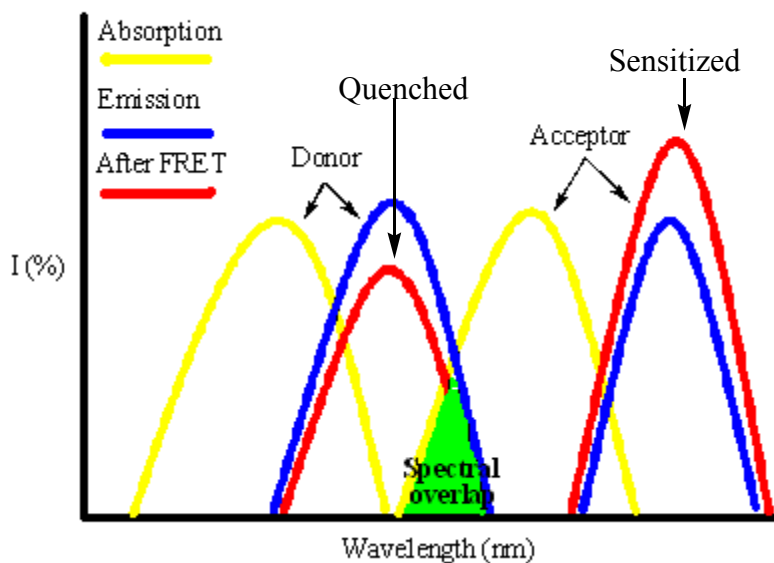


Figure 4. A schematic representation of the donor and acceptor absorption and emission spectra for application as a FRET pair.

To choose a pair of chromophores for a FRET study, their excitation spectra must have enough separation for selective excitation of the donor. Also, there must be enough separation in the emission spectra, to allow measurement of emission from each fluorophore independently. Generally the pair needs to have an overlap greater than 30%. In measuring short distances, less than 20 Å, the pair needs to have a short Förster radius. A short R_0 value is characteristic of a

donor and acceptor pair with small overlap, low quantum yield, and a small extinction coefficient. Lanthanide ions are a good example of a small probe, and they have been used to determine distances as small as 3-4 Å.¹ Provided the quantum yield is high, pairs with more spectral overlap are more efficient in measuring long distances, up to 100 Å. The characteristic Förster radius for a pair is derived based on their spectral overlap integral, so the larger the R_0 value, the better the pair. The spectral overlap integral calculation is shown in Equation 5, where f_D is the normalized donor emission spectrum and ϵ is the acceptor extinction coefficient.¹

$$(5) \quad J = \int f_D(\lambda) \epsilon_A(\lambda) \lambda^4 d\lambda$$

The orientation factor κ describes the relative spatial orientations of the transition dipoles of the donor and acceptor chromophores during the excited state lifetime. The dependence of the FRET signal on the relative orientation of the chromophores is one of the method's major limitations in measuring distances. When the transition dipoles are both aligned parallel to the distance vector that connects them, $\kappa^2 = 4$ and the transfer of energy is most likely. If the transition dipoles are orthogonal, $\kappa^2 = 0$ and the transfer of energy will not occur (Figure 5). Usually κ^2 is assumed to be 2/3, which is the value averaged over all angle combinations, and therefore is what will be observed if the chromophores are attached to flexible linkers and are allowed to rotate freely on a time scale faster than energy transfer.

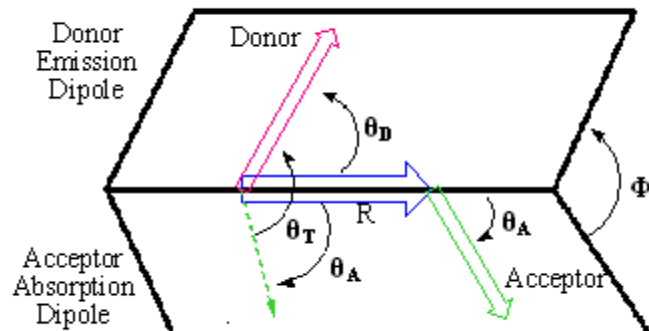


Figure 5. The relative orientation of the donor (θ_D) and acceptor (θ_A) transition dipoles can be described by the distance vector between them (r), the angles formed between r and each dipole, and the angle between the two planes containing the transition dipoles (Φ): $\kappa^2 = (\sin \theta_D \sin \theta_A \cos \Phi - 2 \cos \theta_D \cos \theta_A)^2$.

In situations where the chromophores may not be able to undergo rapid and random rotation, for example, when chromophores are attached to a biological membrane or in a viscous solution, the uncertainty in κ^2 leads to increased error in calculating R_0 .^{2,7,9} The uncertainty increases with increasing size of molecules or proteins, or those with multiple linkages, and the assumption that κ^2 is $2/3$ is only accurate for small peptides and proteins. This dependence on rapid rotation can give uncertainty in measurements of distance up to 35%. When they are unable to rotate freely, the efficiency will depend on their initial orientation. To overcome this obstacle, we propose the synthesis of tetrahedral and pseudotetrahedral assemblies of chromophores that will ensure an isotropic system and a κ^2 value of $2/3$.

II. Project Design

Our project is to design three-dimensional chromophores that have isotropic absorption and emission spectra, and will thus eliminate the uncertainty caused by the orientation factor. These tetrahedral chromophore arrays will consist of known organic dyes as the building blocks, symmetrically attached to a silane core as shown in Figure 1.

The history of synthetic dyes dates back to the late 1800s. Although many were highly colored, like methyl violet and malachite green, they were weakly fluorescent and could not be used in today's application as fluorophores. However, some of the dyes from that period turned out to be highly fluorescent and are the forefront of the fluorescent probes used in modern microscopy. One example is the substituted xanthene family that includes fluorescein and rhodamine B.³⁹

Over the past sixty years, the introduction of fluorescence microscopy, the discovery of naturally occurring fluorescent proteins and the recent development of fluorescent semiconductor quantum dots have opened the field to new research opportunities. Despite recent advances in synthesis of traditional fluorescent dyes, there is still little known about the specific molecular properties responsible for generating the optimal characteristics for fluorescence. Current development

of novel probes is difficult and uses what is known from existing dyes' properties in attempt to design a structure that can be used with available confocal laser excitation wavelengths. Therefore, there are thousands of fluorophores that have been discovered that one can choose from.^{6,39}

There are many characteristics that are important for fluorophores, including their spectral profiles and fluorescence intensity. A useful quantitative parameter is the molar extinction coefficient, which measures the ability of the molecule to absorb light. Another measure is the quantum yield of the fluorochrome, given in a range from 0 to 1. A high yield is desired and can vary depending on environmental factors, such as concentration, pH, and solvent. In microscopy studies, it is important to look at the spectral lines needed to excite the fluorophore most efficiently. For FRET applications, the donor needs to have an absorption maximum close to a laser spectral line, as the intensity of fluorescence emission is regulated by the fluorophore extinction coefficient at the excitation wavelength. The most used lasers are argon and krypton-argon ion, the blue diode laser, which has a 488 nm line.³⁹

Some of the advances in design of synthetic organic dyes can be seen by the Alexa Fluor dyes introduced by Molecular Probes. They are sulfonated derivatives known for having higher quantum yields, enhanced photostability, pH insensitivity, and are highly water soluble. Sulfonation makes the dyes negatively charged and hydrophilic. They are named based on their absorption spectra

matched to common laser lines. The dyes are available in a large range of excitation and emission wavelength, covering the full range of the visible spectrum and going into the infrared. They are commercially available as reaction intermediates, such as maleimides, succinimidyl esters and hydrazides in the 5 or 6 position of the benzene moiety. Some of the xanthene derivatives are shown in Figure 6.³⁹

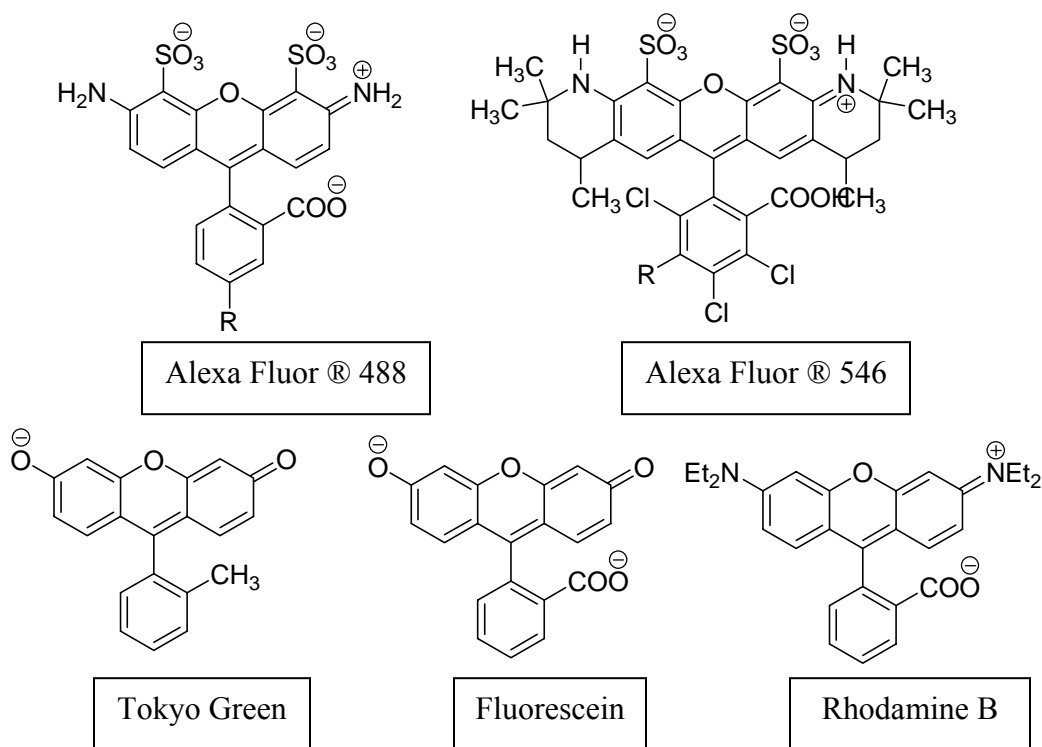


Figure 6. Examples of organic dyes from the xanthene family.

Also in the xanthene family, fluorescein is one of the most wide used fluorophores ever designed. The dye has an absorption maximum at 492 nm,

which corresponds well with the spectral line of 488 nm from the argon-ion and krypton-ion lasers. The quantum yield is very high, at 0.85, but the emission intensity depends greatly on environmental factors like changes in pH. It has been found that xanthene dyes are susceptible to hydrogen bond effects. Rhodamine B has a tunable wavelength around 610 nm and its quantum yield is dependent upon temperature. Since the emission maximum of fluorescein is around 520 nm and the absorption of rhodamine is 510, they have sufficient spectral overlap to be used as a FRET pair. Rhodamine B is commonly used due to the fact that it is insensitive to pH changes, more water soluble and more stable to photobleaching than fluorescein.^{2,6,14}

Using a known organic dye as the building block for the array will enable us to benefit from the advantages of these chromophores, yet remove the orientation dependence that creates uncertainty in the measurement. For the organic dye that would serve as a building block of the array, rhodamine B was initially chosen for proof of concept. Since fluorescein and rhodamine both have well-defined transition dipoles, the chromophore orientation can be controlled through molecular design. In addition, the rhodamine or fluorescein structure can be modified to eventually link the array to the biomolecules for study. The initial synthetic goal was therefore to prepare tetrakis(rhodamine)silane **2**.

In our tetrahedral arrays, each individual chromophore is very close to the others. The chromophores may interact by two possible mechanisms, intra-array

FRET or true quantum coupling. When one of the chromophores within the array absorbs a photon, the question is whether there is scrambling of the excitation to each chromophore faster than the energy can transfer to an external chromophore. Previous studies by Goodson and coworkers¹⁵ found that energy transfer will follow an intra-array FRET mechanism. Using a tetrahedral compound, consisting of an adamantane core and styrylstilbene chromophore arms, FRET was observed to occur intramolecularly on a sub-picosecond timescale (Figure 7). For our project, this rapid intra-array FRET will occur when one of the chromophores is excited, so the array will appear to an acceptor as a single, spherical chromophore. The effect will be similar to a single planar chromophore rapidly rotating. This rapid FRET is important in maintaining isotropic emission for our arrays.

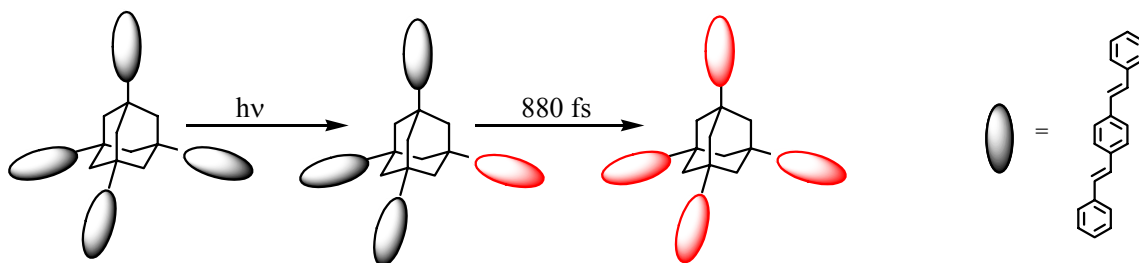


Figure 7. Goodson and coworkers found that intra-array FRET occurs on a sub-picosecond timescale. (Black oval is ground-state chromophore and red is excited chromophore)

Our system will utilize chromophores with structures that can be divided into two parts that are orthogonal to each other, as seen in Figure 8. The π

systems of the xanthene moiety, which plays the part of the fluorophore, and of the benzene moiety do not have any significant ground-state interaction. Therefore, our array can be considered as four fluorophores on a tetraaryl core. We have considered three possible cores; silane, adamantane, and methane. They all can provide a tetrahedral arrangement of the chromophores, yet remain small enough to be able to obtain accurate distance measurements. We decided to focus first on the silane core because it appears to have the most straightforward synthesis and because it is smaller than adamantane, which will decrease the overall size of the array.

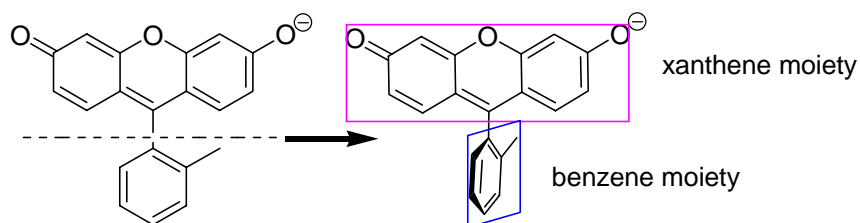


Figure 8. Tokyo Green structure divided into its two parts, the xanthene and benzene moieties.

To use our arrays in FRET studies, the size of the arrays must not add any new uncertainties in distance measurements. In comparing our arrays to an individual chromophore, the array is much larger. The proposed assembly is predicted to have a diameter of 1.5 to 1.8 nm. The diameter of an individual fluorescein along its dipole is only 0.9 nm. However, this difference in size should have little effect, since FRET measurements are only accurate when the

traditional chromophore is rapidly rotating around its point of connection. The array's cross-section is therefore comparable to the size of an individual chromophore rotating, which would cover approximately the same area of 1.7 nm.

The proper core will separate the individual chromophores enough to prevent electronic coupling interactions between them, so that each of the planar chromophores would maintain their absorption and emission energies. Yet the size of the chromophore array needs to be similar to that of a single chromophore rotating around its flexible linker. Nancy Goroff performed semi-empirical quantum calculations (PM3) and found that using silane as a core would place the chromophores close enough for rapid FRET to occur and achieve isotropicity, yet far enough apart so that they remain electronically independent of one another (Figure 9 and 10). If the chromophores experience any quantum coupling their emission and absorption energies may be altered, rendering them unsuitable for studies using FRET. Using a pseudotetrahedral array with rhodamine B chromophore units, it was found there is no electronic coupling between the individual chromophores and almost no electron density was observed on the benzene moieties. The calculated HOMO-LUMO energy gap on an individual rhodamine B in the array is 0.27 eV, whereas an isolated rhodamine B is 0.26 eV.

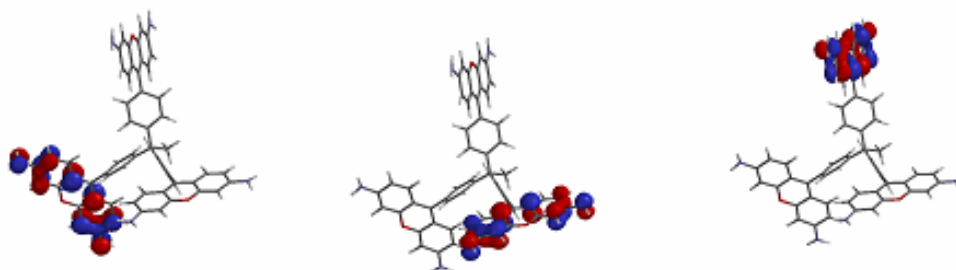


Figure 9. The three degenerate HOMO's, each localized on one of the chromophores, for a pseudotetrahedral array of three rhodamines on a silane core (PM3 calculation).

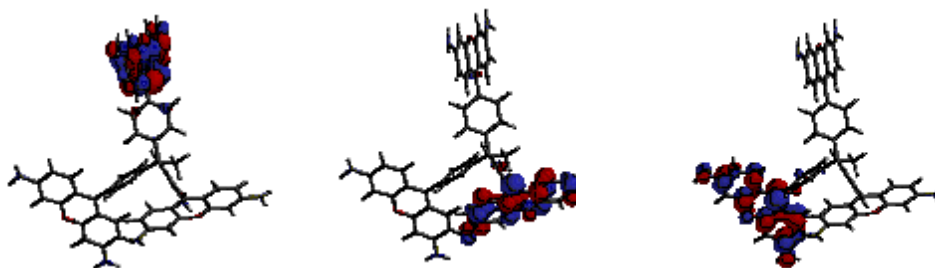


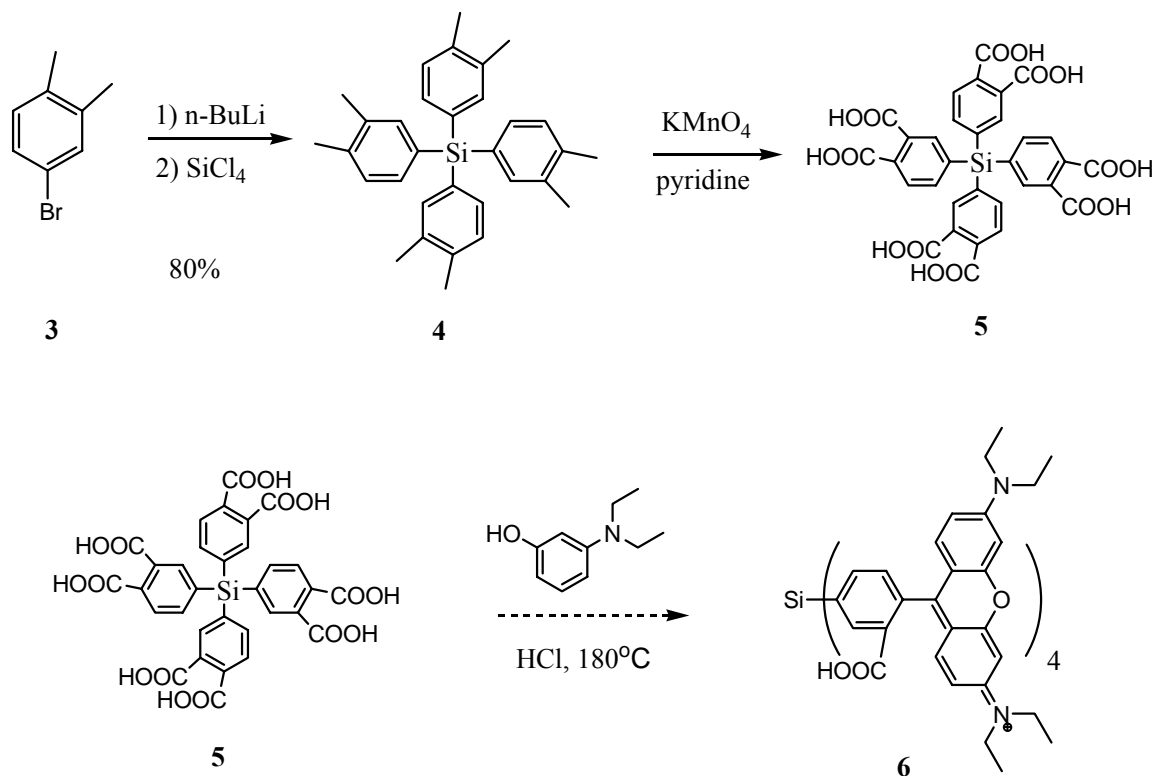
Figure 10. The three degenerate LUMO's, each localized on one of the chromophores, for a pseudotetrahedral array of three rhodamines on a silane core (PM3 calculation).

III. Synthesis

We have developed three synthetic routes to the chromophore array. The first strategy was to build the chromophores up on the central silane core (Scheme 1). The second strategy, carried out in conjunction with Lu Zhou, was to prepare the chromophores individually and attach them all at once to the core (Scheme 2). The third route, described in this thesis, focuses on synthesizing the xanthene unit of the chromophore and then coupling it to a tetraaryl moiety using a Grignard reaction.

A. Strategy 1

The first strategy was attempted by previous group member Lu Zhou, using rhodamine B as the chromophore with the three dimensional array **6** as the target.³⁸ Since rhodamine B can traditionally be made using two equivalents of aminophenol in a reaction with phthalic anhydride at increased temperature, the octa-acid **5** was the initial target.



Scheme 1. Proposed synthesis for building the chromophores up on the silane core.

Organo-lithium reagents, such as n-BuLi, have been found suitable to prepare fully substituted silanes.²⁶ Using the same method, tetrakis-(3,4-dimethylphenyl)silane **4** was successfully prepared. Oxidation with potassium permanganate gave the desired octa-acid **5**. However, the final step to form the rhodamine B array proved difficult. Although reaction led to the appearance of a deep pink color, consistent with formation of rhodamine B, purification using column chromatography and recrystallization were not successful.

The problems faced in isolation could be caused or amplified by the possibility of two different isomers and multiple charged states for rhodamine B (Figure 11).²¹ Also, the strategy requires the final reaction to occur in high yield at all four sites on the silane. Partially substituted products and isomers will both create difficulty when it comes to purification of the final array by this strategy.

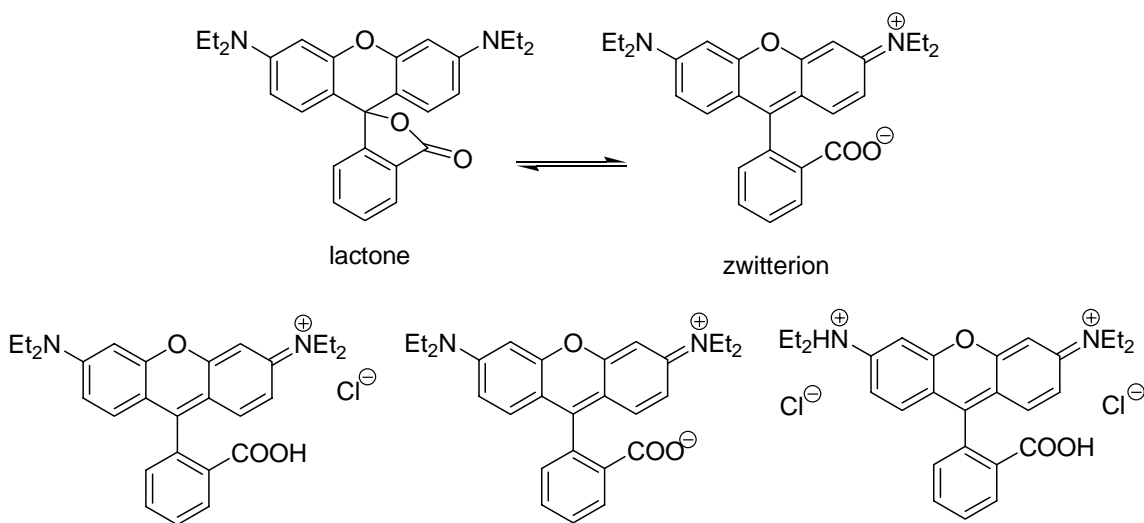


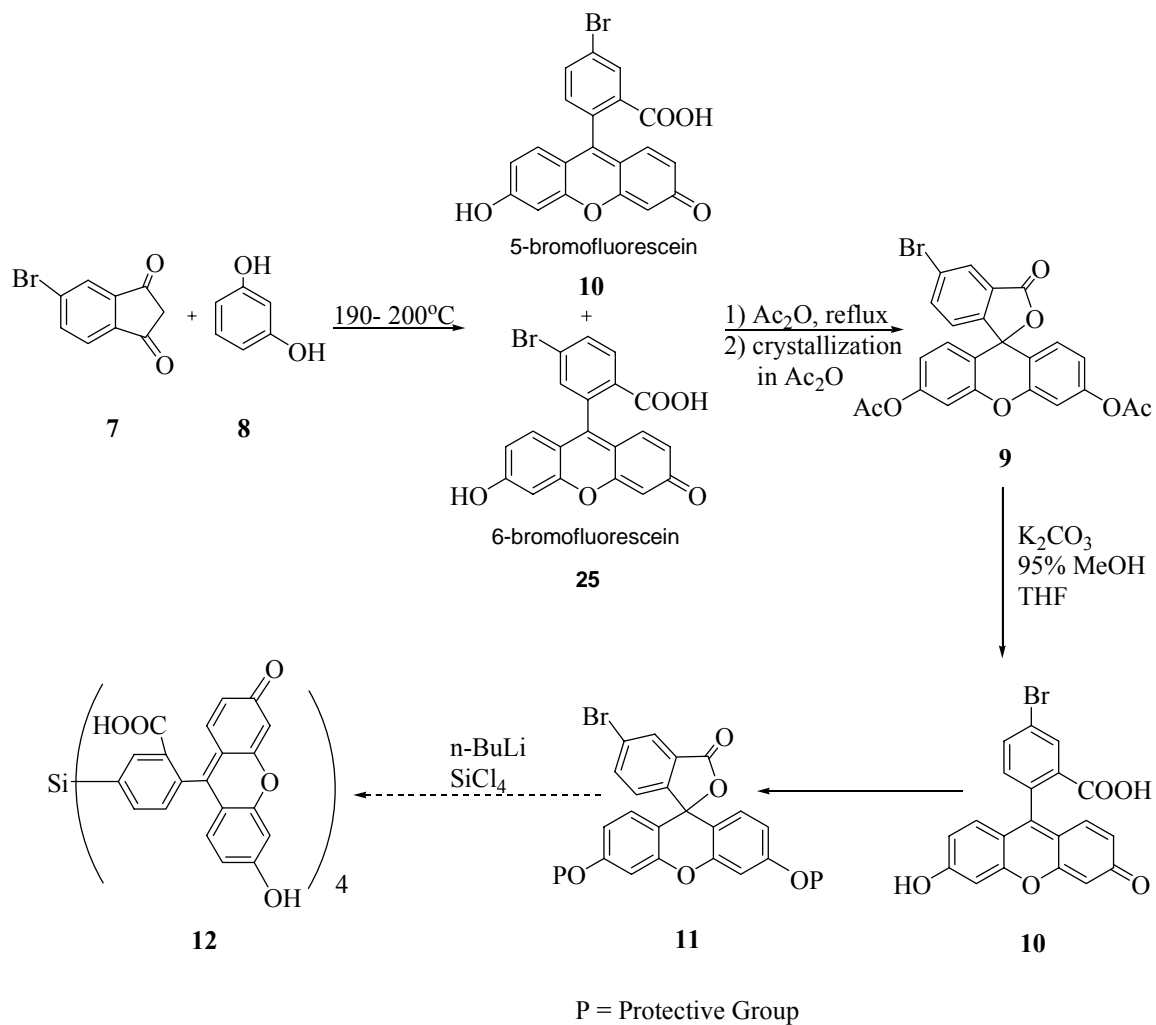
Figure 11. The two principle isomers of rhodamine B and charged states that are possible.

B. Strategy 2

For the second route, rhodamine B must be prepared first and then attached to the silane core. Since rhodamine B has functional groups that will react with n-BuLi, it could not be attached directly and would need protecting groups for the final step. Due to obstacles in the previous strategy and problems

finding suitable protecting groups, the scheme was altered to synthesize fluorescein.

The first goal was to synthesize 5-bromofluorescein **10**, to attach the chromophore later to the core (Scheme 2). Lu Zhou successfully prepared compound **10** starting from resorcinol and 4-bromophthalic anhydride. The reaction also forms the regioisomer, 6-bromofluorescein **25**, but the desired compound **10** can be purified using fractional crystallization after forming the diacetate derivative.²² The acetate protecting groups are easily cleaved by adding potassium carbonate to a solution of compound **9** in methanol.



Scheme 2. Proposed synthesis for preparing the chromophores and then attaching them to the silane core.

Since fluorescein also has functional groups that will react with n-BuLi, appropriate protecting groups are needed to protect the phenol groups. The carboxylate group is protected by forming a lactone ring at the same time. Model

reactions were performed using protected fluorescein, to observe whether the protecting groups remained after being treated with the harsh conditions of n-BuLi. It has been found that very few protecting groups can withstand n-BuLi conditions. Phenol protecting groups are cleaved more readily than other alcohols. Possible protection groups to be tested include: methyl ethers, silyl ethers such as trimethylsilyl (TMS), t-butyl-dimethylsilyl (TBS), and triisopropylsilyl (TIPS) ether, and acetals such as methoxymethyl (MOM) ether.²³

Lu Zhou prepared both the di-butyl fluorescein and the bis (TIPS) fluorescein.²⁸ She found that when the butyl protected fluorescein was exposed to BuLi at -78 °C, the butyl protecting groups are immediately eliminated. A TIPS protected phenol group was expected to be stable under organolithium conditions, but when n-BuLi was added to a solution of the diTIPS fluorescein, the protecting groups were again cleaved after several minutes. In more recent efforts, we tried to avoid this problem by using a milder base, phenyllithium. When using lithium metal and bromobenzene and adding to it a solution of the protected fluorescein, we again observed the cleavage of the TIPS groups as the temperature was allowed to rise. However, unreacted bromobenzene was observed by TLC, so the Grignard formation was not complete and the protected fluorescein was exposed to a mixture, including lithium metal. The TIPS protected fluorescein experiment in phenyllithium conditions needs to be carried out in the future.

C. Strategy 3

The final strategy involves the synthesis of the xanthene and benzene units of the chromophore separately before forming the desired array. We have decided to focus on the chromophore Tokyo Green, which is a fluorescein derivative, but does not have the added complication of a carboxylate group on the benzene moiety.¹⁶⁻¹⁸

Tokyo Green, which contains a methyl group in place of the carboxylate, was recently reported by Urano and coworkers. It was found to have very similar emission and absorption to fluorescein and has the same fluorescence efficiency (Figure 12). Earlier work by Lindqvist and coworkers reported that the carboxylic acid group was needed for fluorescein to maintain its quantum efficiency.²⁹ However, the Urano group found that the polarity of the carboxylate is unimportant and it can be replaced by methyl.

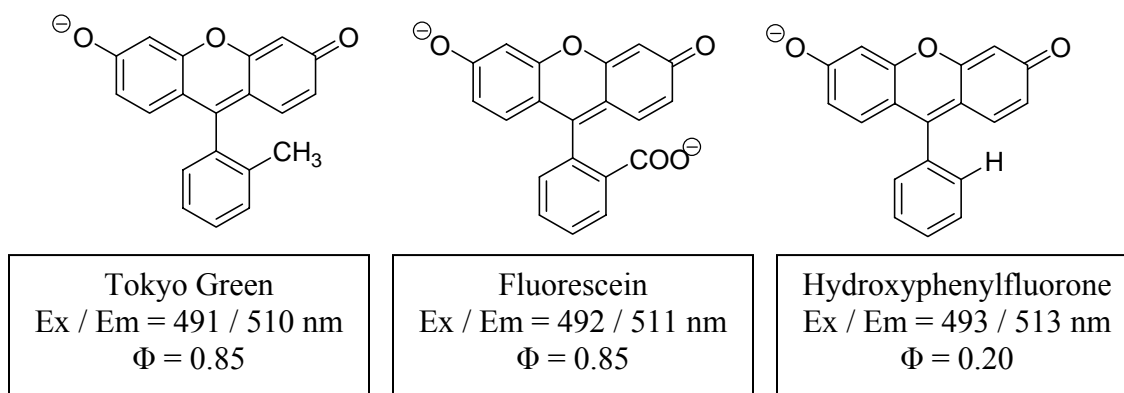
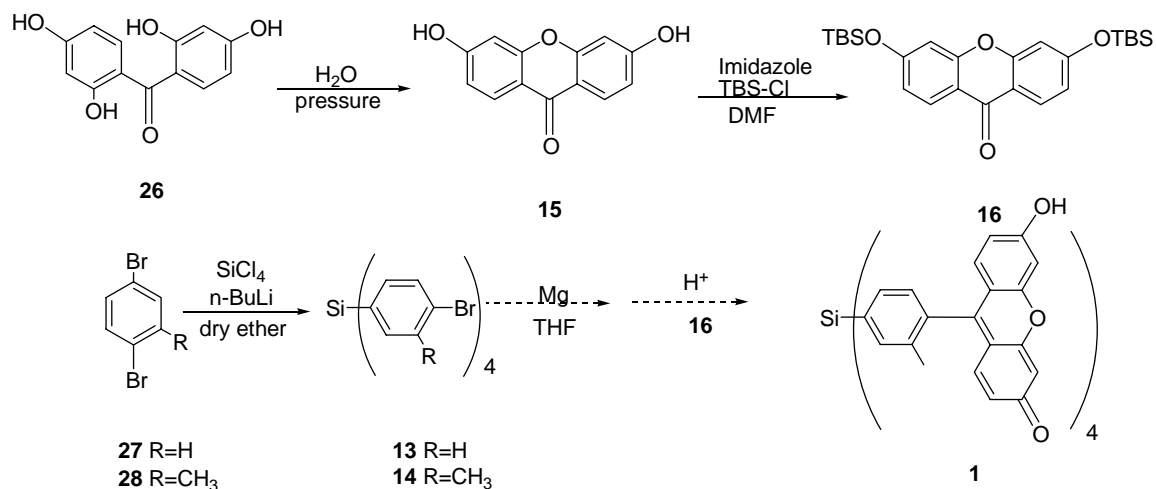


Figure 12. Effects on fluorescence properties due to substitution on benzene moiety.

The xanthene moiety acts as the fluorophore and the methyl group helps to keep the two parts orthogonal to one another. As we found in the PM3 calculation, the two units have little or no interaction in this orientation. Urano and coworkers found a hydrogen atom is not sufficient to force orthogonality, which is why hydroxyphenylfluorone has a quantum yield of only 0.20. The Urano method for preparing Tokyo Green uses the reaction of an aryl Grignard reagent with a TBS-protected xanthene. Our strategy is to allow the TBS-protected xanthone **16** to react with tetrakis(bromotoluy)l)silane **14** by Grignard coupling (Scheme 3). The advantage of this scheme is that there are no harsh conditions needed to connect the xanthene and aryl moieties. The final step is reported to take place in high yield, which should simplify the purification of the final array.



Scheme 3. Proposed method for preparing the xanthene and aryl moieties and then attaching them through Grignard coupling.

i. Synthesis of xanthene moiety

To prepare the bis-TBS xanthone **16**, we followed reported procedures (Scheme 3).^{31,33} The first step involves heating 2,2',4,4'-tetrahydroxybenzophenone **26** in water in a pressure tube to 195-200 °C to give 3,6-dihydroxyxanthone (**15**), which is also commercially available. When Lu Zhou carried out this reaction previously, she obtained very low yields. Because the xanthone **16** is needed in high excess in the final coupling reaction, it was important to increase the yield of this reaction before the protection step. According to the literature, the reaction requires only 2 hours at 200-220 °C. Lu

Zhou had performed the reaction at 180 °C for 4 hours to get a yield below 10 %.

We then repeated, but heated the mixture in a silicon oil bath at 195-200 °C.

The difficulty comes when trying to purify the xanthone **15**. The starting material is soluble in hot water, but simply filtering and washing the product does not remove all the starting material. The filtered solid was also heated in refluxing water, filtered, and then dried in the vacuum oven. The NMR still showed peaks corresponding to benzophenone **26**, so a new method was tried to separate xanthone **3** from the starting material. A soxhlet extraction was performed using distilled water as the solvent. The water in the round- bottom flask turned yellow from dissolved benzophenone **26**, and after 2 days the extraction resulted in pure xanthone **15** left in the thimble. However, there was also an unknown solid precipitate in the water below. After NMR analysis the unknown was found also to be the xanthone product **15**.³¹

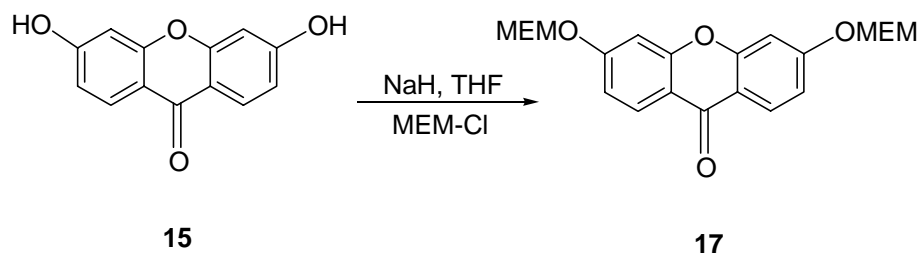
Because of the loss of material in the soxhlet extraction, the reaction was carried out again. Another possible reason for the poor results was that the pressure in the tube was not high enough for the cyclization to occur at the high yields that were previously reported. Therefore, the reaction was carried out again, this time with twice as much starting material as before. The reaction proceeded for 6 hours before filtering, washing, and heating in water to reflux to remove the starting material. The yield of 23% was still low, but had more than

doubled from the previous attempts, and we had enough material to continue to the next step.

The t-butyldimethylsilyl (TBS) group had previously been found successful to protect the two hydroxyl groups of xanthone **15**.¹⁶ The xanthone bis-TBS ether **16** was prepared using imidazole and t-butyldimethylsilyl chloride (TBS-Cl) and letting the reaction proceed for about 48 hours, much longer than the 2 hours reported in the literature procedure.³³ TLC (1:3 hexane/ethyl acetate) after 4-5 hours showed two spots; one is thought to be the mono-substituted product and the second is the starting material, xanthone **15**. Over time, more of the bis-substituted product **16** formed. The product was an oily solid after work-up, which was then recrystallized from chloroform and ethanol. The proton NMR of the recrystallized product was consistent with the desired TBS-protected **16**.

We repeated the reaction to obtain more material, following the same procedure, but during the extraction an emulsion formed. The solid material was separated from the solvent by gravity filtration, and TLC and NMR showed it to be the starting material **15**. Using the recovered starting material, the procedure was repeated again, paying careful attention to add everything through a cannula, keep it under argon, and drying the starting material **15** thoroughly in a vacuum oven. This extra caution proved to be effective, and the reaction was successful. After recrystallization twice, the bis-TBS xanthone **16** was pure by to NMR.

We also synthesized MEM- protected xanthone **17** (Scheme 4). Peterson and coworkers have found the MEM protecting group to be effective for the preparation of the Tokyo Green derivative, Pennsylvania Green.³⁴ The reaction to synthesize 3,6-dihydroxyxanthone **15** was repeated and the yield was increased to 33%. Once xanthone **15** was purified and dried, the Peterson procedure for the addition of MEM groups was followed on a 100- mg scale (Scheme 4). The xanthone **15** was dissolved in dry THF and the temperature was brought down to 4 °C before adding NaH. After the mixture stirred for half an hour, the MEM-Cl was added, and the mixture was allowed to warm to room temperature over a period of 20 hours. After work-up and column chromatography, the product was further purified by recrystallization from chloroform/ethanol to give 112 mg of pure protected xanthone **17** as white crystals in 65 % yield.



Scheme 4. Reaction to synthesize 3,6-Bis-(2-methoxy-ethoxymethoxy)-xanthone-9-one **17**.

ii. Synthesis of tetraaryl silane core

Lu Zhou modified the literature procedure for the preparation of tetrakis(bromophenyl)silane **13** to synthesize **14**, using the commercially available 2,5-dibromotoluene and tetrachlorosilane.³² After two successive recrystallizations using a chloroform/ethanol solvent pair, the tetrakis(4-bromo-2-methylphenyl)silane **14** was obtained. The structure of compound **14** was confirmed by ¹H and ¹³C NMR and X-ray crystallography (Figure 13).³⁸ Because preparation of silane **14** requires four successive selective reactions with dibromotoluene, the isolated yield was only 10 %.

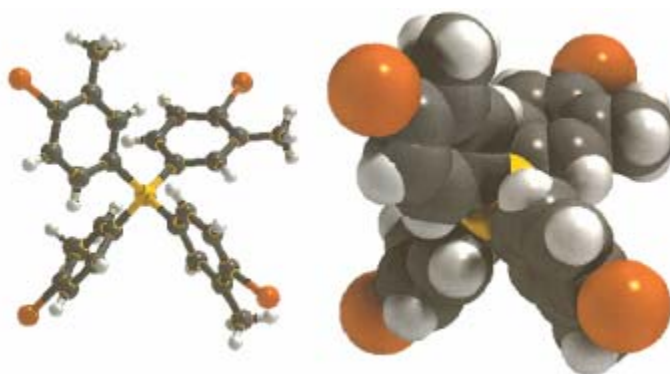
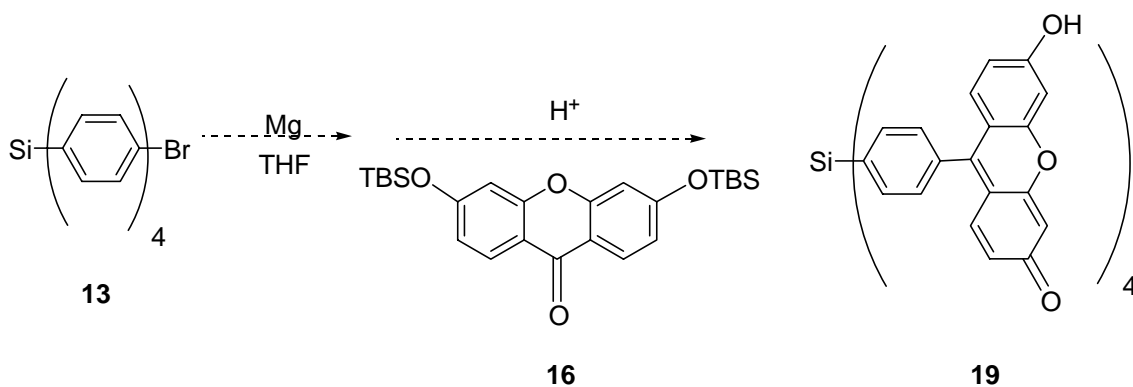


Figure 13. Crystal structure of tetrakis(4-bromo-2-methylphenyl)silane **14**.

iii. Model Reactions to couple xanthone and aryl moieties

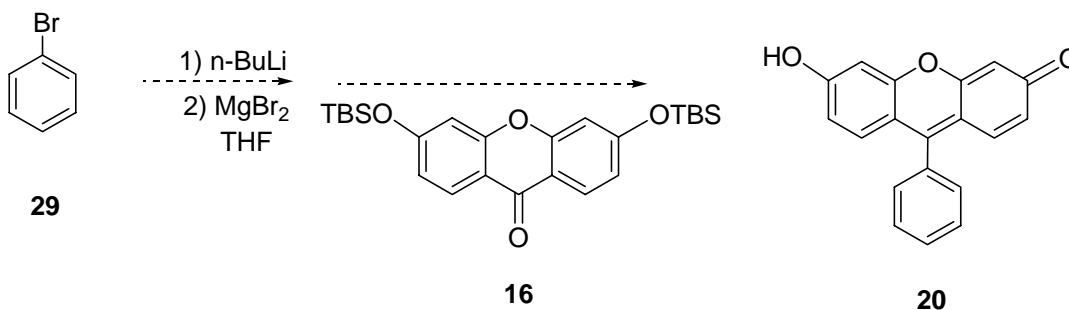
Once we had successfully synthesized both starting materials, we attempted to modify the literature procedure for the synthesis of the Tokyo Green

fluorophore, to prepare model tetrahedral array **19** (Scheme 5).¹⁶ For this model, we used tetrakis(bromophenyl)silane **13** as the bromobenzene substrate to test our ability to carry out reaction four successive times. The procedure uses magnesium metal turnings, which are dried under argon before adding the aryl derivative to form the Grignard. Xanthone bis-TBS ether **16** was added to the Grignard mixture, and the reaction was quenched with hydrochloric acid solution after the solution stirred 15 minutes. The resulting precipitate was filtered and analyzed by NMR. The NMR analysis showed both starting materials, the bis-TBS xanthone **16** and the tetrakis(bromophenyl)silane **13**, and some unknown peaks. But there were no peaks in the range we would expect for our desired product. The TLC's also confirmed both starting materials in the filtrate. The presence of both starting material suggests there was no formation of the Grignard reagent.



Scheme 5. Model Reaction 1.

The results of this attempt were difficult to interpret due to the possibility of partial reaction of the silane. In addition, because the desired transformation requires the Grignard reaction to happen four times on each silane, it required a large amount of the protected xanthone **16** starting material. To make sure the Grignard reagent does form, we decided to carry out model reactions to find the proper reaction conditions. Although 2-bromotoluene seemed to be the best model, the reagent was initially unavailable, so bromobenzene was used first.



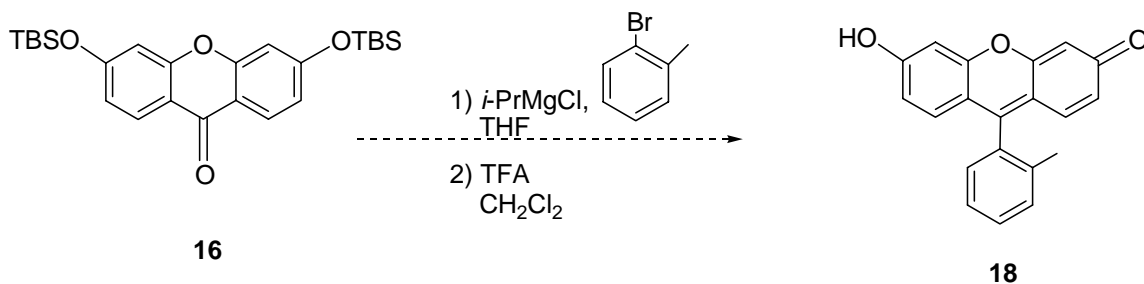
Scheme 6. Model Reaction 2.

After the synthesis of more xanthone **15** and bis-TBS xanthone **16**, a different method was attempted to form the desired product. Using bromobenzene **29**, n-BuLi was added to lithiate at the bromine position, and then magnesium bromide was added to form the Grignard reagent (Scheme 6). Finally, the bis-TBS xanthone **16** was added via cannula to complete the reaction. The TLC showed there was still bis-TBS xanthone **16** in the resulting mixture after quenching. There was no indication of bromobenzene by TLC. After

workup, the product mixture included both solid and oil components. A ^1H NMR spectrum of the solid showed only the starting material, bis-TBS xanthone **16**. The ^1H NMR spectrum of the liquid contained peaks corresponding to the protected xanthone **16** and other unknown peaks, but none corresponding to the bromobenzene starting material. TLC of the liquid showed four spots: one corresponding to the xanthone, one that only showed up when stained with PMA (dark spot), one that was visible under short wavelength UV light, and one that was visible under long wavelength UV and appeared as a white spot after dyeing. A gradient column (hexanes \rightarrow hexanes: ethyl acetate \rightarrow methanol) was then used to separate the spots. The column resulted in the separation of five fractions, but the identification of six components. The third and fourth components came out at the same time and could not be separated. NMR was taken for all five separated fractions, but the only identifiable material was Fraction 1, bis-TBS xanthone **16**. The NMR data did not support formation of the desired product.

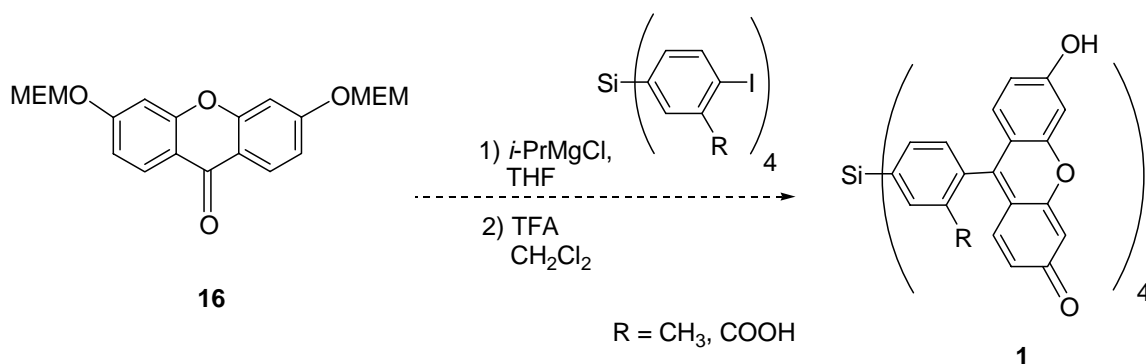
Since the two model reactions did not look promising, the next step was to try a method that recently was published to synthesize the fluorophore Pennsylvania Green (Scheme 7).³⁴ Peterson et al. synthesized a MEM-protected xanthone and allowed it to react with the Grignard reagent made from 2-iodotoluene and *i*-PrMgCl. For our model reaction we used *i*-PrMgCl and 2-bromotoluene, to test the efficiency of this method to attach the aryl moiety to the

xanthone. The product of this model reaction would be the fluorophore Tokyo Green.



Scheme 7. Model reaction 3 to synthesize Tokyo Green.

Our model reaction was carried out by mixing 2-bromotoluene and *i*-PrMgCl in THF under argon, to undergo a halogen-metal exchange. After two hours at room temperature, the bis-TBS xanthone **16** was added. The reaction mixture turned an orange color and then faded to bright yellow, and was allowed to stir for 19 hours. The reaction was quenched with methanol and the solvent was removed *in vacuo*. The resulting yellow residue was redissolved with CH₂Cl₂ and treated with TFA. After an additional 2 hours the solvent was removed again and a crude NMR was taken. NMR analysis showed the presence of the starting materials 2-bromotoluene and bis-TBS xanthone **16** and did not match what is expected for Tokyo Green, again suggesting there was no Grignard formation.

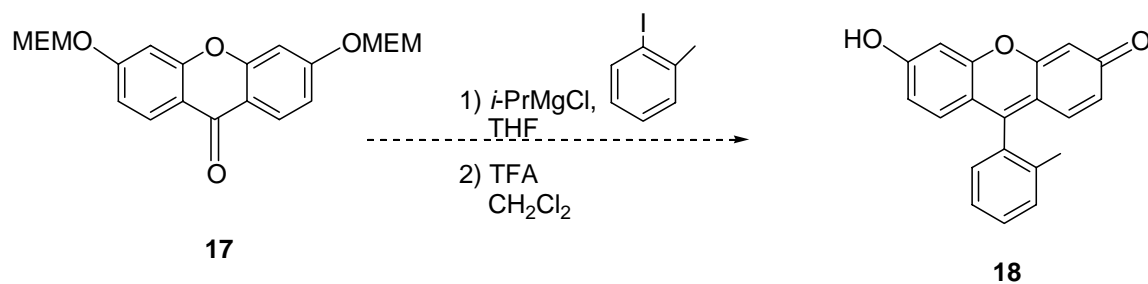


Scheme 8. Proposed reaction to synthesize array 1.

The next step was to try the model reaction modified from the Peterson procedure to make Tokyo Green (Scheme 9).³⁴ 2-Iodotoluene and *i-Pr*MgCl were allowed to react at room temperature for 2 hours, followed by addition of the bis-MEM xanthone **17**, immediately turning the solution orange-red. The mixture was stirred for an additional 18 hours. At that time the solution, which was opaque and yellow, was quenched with methanol. The solvent was removed, and the residue was dissolved in CH_2Cl_2 and treated with TFA, where upon it turned darker in color. After 30 minutes the solvent was removed again, but the product never became a fully dry solid.

A crude NMR showed impurities, so a column was carried out following the literature procedure, using a solvent mixture of 1:20 methanol/ CH_2Cl_2 . But, the mixture was too polar and several spots came out together without separation. By TLC there were more than five spots; several dyed the plate yellow and were

brightly yellow fluorescent under UV light. We tried to find a suitable mixed solvent, in which the yellow spots would be kept on the baseline, so an additional column could be used to remove additional impurities. But these efforts were unsuccessful, so recrystallizations were attempted. Unfortunately, the sample was not fully soluble in any solvent but DMSO. Tokyo Green is reported as being soluble in methanol, but the sample was only slightly soluble, and a red powder would always fall out of solution. ^1H NMR of the red powder proved difficult because of its poor solubility. If the reaction did form the desired Tokyo Green, it did so only in small yield, and therefore would not be well suited for the final step in the synthesis of the array, which needs to be a very high yielding reaction.

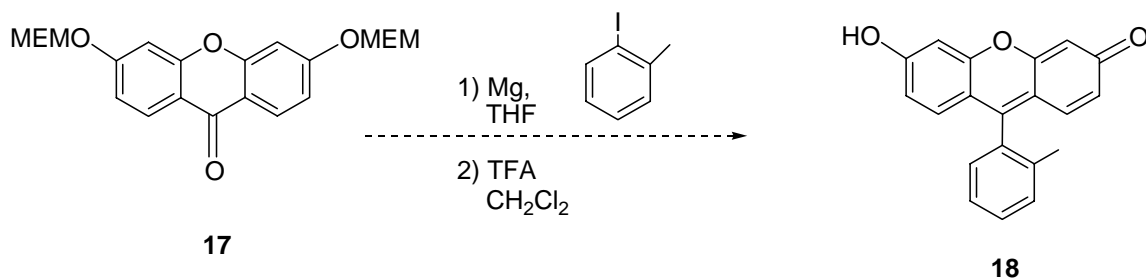


Scheme 9. Model reaction 4 to prepare Tokyo Green.

After speaking to a member of the Peterson group about their methods, we decided to carry out Model Reaction 5 as a standard Grignard reaction using magnesium metal and 2-iodotoluene (Scheme 10). Extra precaution was taken to

ensure there was no water in the reaction. The bis-MEM xanthone was dried in the vacuum oven with P_2O_5 and the Mg turnings were dried in the oven overnight. To a flame-dried round-bottom flask containing the dry Mg, 2-iodotoluene dissolved in dry THF was added and allowed to reflux for 2 hours. Once cooled to 0 °C, the bis-MEM xanthone was added via cannula and stirred as it warmed up to room temperature overnight. The solution was opaque and white in color before quenching with MeOH.

Before the deprotection step with TFA, we wanted to purify the sample to decrease the number of impurities, compared to the previous model reaction. Column chromatography using a solvent mixture of 1:20 MeOH/ CH_2Cl_2 was successful in the separation of three fractions. The components were difficult to analyze by 1H NMR because the MEM protected xanthone starting material has very similar peaks to what is expected for the protected chromophore. Thus, the two promising fractions were allowed to react separately with TFA and then analyzed by 1H NMR. One of the fractions looked promising. Upon reaction with TFA, the solution turned yellow-orange in color, and by 1H NMR there were new aromatic peaks in the range expected for Tokyo Green. As there were still obvious impurities by TLC and NMR, another column was run, using a UV lamp to observe the fluorescent bands to aid in the separation. Although three brightly colored fractions were separated, NMR analysis showed that none of the fractions contained aromatic protons in the expected range.



Scheme 10. Model reaction 5 to prepare Tokyo Green.

The most promising results, thus far, were using *i-Pr*MgCl and 2-iodotoluene to form the Grignard (Scheme 9). In the previous attempt, not as much care was taken to keep the reaction conditions free of water, which may have resulted in the large number of byproducts. The procedure was repeated, taking extra precautions to dry the xanthone in the vacuum oven for several days and using NMR to make certain there was no water remaining. Protected xanthone **17** was placed under vacuum overnight, and also flame-dried while connected to the vacuum pump. When the xanthone was added to the flask containing 2-iodotoluene and *i-Pr*MgCl in dry THF, the solution immediately turned yellow. After the reaction was allowed to stir overnight, the following morning there was no longer any liquid in the flask; only a light yellow solid remained. From TLC, the sample showed as only one spot. Difficulty arose when finding a suitable solvent to take the NMR. The sample was found to be

soluble in CD₃OD when heated, but fell out of solution as the NMR was taken. The NMR included low-intensity peaks in the aromatic region, so we performed the TFA deprotection. Upon addition of TFA, the solution turned orange. However, after the deprotection, the product NMR included no peaks in the range from 7.1-7.6 ppm that would belong to Tokyo Green.

iv. Successful coupling to form Tokyo Green

We wanted to try once more the model reaction to prepare Tokyo Green using Mg turnings and the bis-MEM xanthone (Scheme 10). Knowing that water greatly hinders Grignard reactions, every preventative measure was taken to keep it out. The bis-MEM xanthone **17** was weighed out in slight excess. It was dissolved with CHCl₃ and rotovapped to spread the sample evenly on the sides on the round-bottom flask. The magnesium metal was also weighed and both were dried in the vacuum oven for three days with fresh P₂O₅ at 80 °C. The reaction flask was flame dried under vacuum and allowed to cool before turning on the argon supply and adding the dried magnesium turnings. The flask was then flame dried again under vacuum. All needles used in carrying out the reaction were dried in the oven and cooled in a dessicator.

In carrying out the reaction, dry THF from a fresh still was added to the magnesium metal, along with an excess of 2-iodotoluene. The mixture was

allowed to heat at reflux under argon for 2 hours and bubbling was observed, indicative of Grignard formation. When the flask containing xanthone **17** was taken out of the oven, it was stoppered and then put straight on the vacuum pump and flame-dried. The Grignard flask was allowed to cool, and the solution turned cloudy with white solid at the bottom of the flask. Bis-MEM xanthone **17** was dissolved in THF and added to the reaction flask via cannula at 0 °C, whereupon the solution turned yellow. The reaction was allowed to warm to room temperature overnight and then quenched with MeOH. The solution turned from grey and cloudy to yellow and clear. The leftover Mg turnings were bubbling intensely, so 2 M HCl was added to quench the magnesium. The solution immediately turned yellow and then orange, which is thought to be due to hydrolysis of the MEM groups.

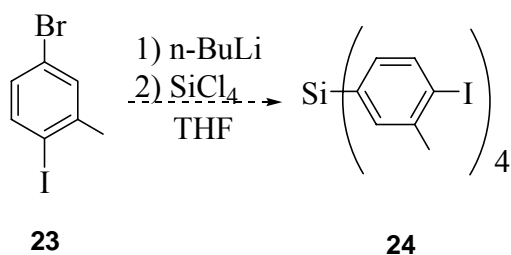
A crude proton NMR was taken in CD₃OD and showed peaks that have not been seen in any of the other model reactions. There proved to be both starting materials, 2-iodotoluene and bis-MEM xanthone, along with deprotected and protected Tokyo Green. TLC indicated multiple spots, one belonging to 2-iodotoluene, and several yellow spots consistent with Tokyo Green, bis-MEM Tokyo Green, and partially protected Tokyo Green. The most nonpolar component, 2-iodotoluene, was removed by a silica plug, using 1:1 hexanes/ethyl acetate.

After another NMR that showed 2-iodotoluene had been successfully removed, the remaining material was dissolved in CH₂Cl₂, and 0.5 mL TFA was added. According to literature, the deprotection should take two hours to be completed.³⁴ After 1 and 2 hours, the reaction flask showed green fluorescence under UV light, indicating that the deprotection was underway. On TLC, the yellow fluorescent spot was becoming less concentrated and the more polar green fluorescent spot was increasing. But after two hours, TLC indicated that the mixture still contained some protected Tokyo Green. The solvent was removed by rotary evaporation and the deprotection step was repeated another two times, adding a little more TFA after two hours and letting it go longer. But, after the third time a faint spot was still observed and it seemed there was still a small amount that was not deprotected. A ¹H NMR confirmed the presence of the Tokyo Green chromophore, but still has slight impurities, which will be removed by column chromatography before final characterization.

v. Proposed new tetraaryl silane core

Because the Grignard reagent is more easily prepared upon reaction with aryl iodides than bromides, the previously prepared tetraaryl silane **14** may not be sufficient. Therefore, the next step of the synthesis is to prepare tetrakis(4-iodo-2-methylphenyl)silane as shown in Scheme 11. We again modified literature procedure for preparing tetraaryl silane compounds from Fournier and

coworkers³², this time using 5-bromo-2-iodotoluene **23** as the starting material. We are unsure if the sterics of the methyl group is enough to deter the n-BuLi from reacting with the iodine first. Our ideal starting material would be 2,5-diiodotoluene. Although this diiodide is commercially available, it is very expensive and we need a large amount due to the expected low yield for this reaction. We therefore started with less expensive compound **23** for our initial experiments.

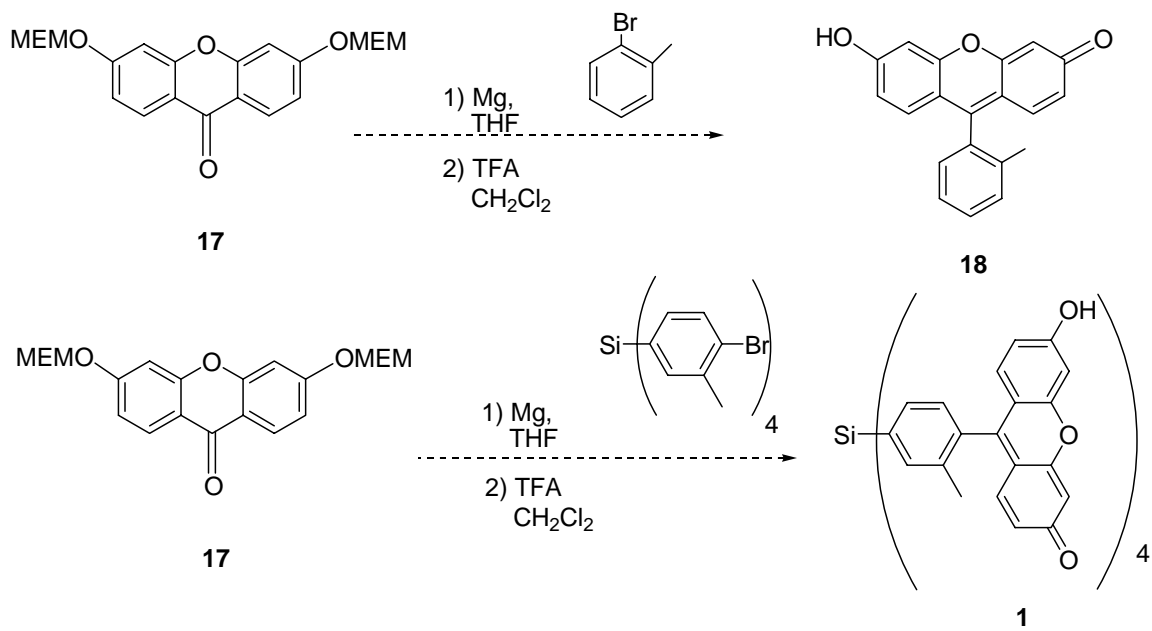


Scheme 11. Synthesis of tetrakis(4-iodo-2-methylphenyl)silane 24.

The reaction was carried out by dissolving 5-bromo-2-iodotoluene **23** in dry THF at -78 °C. The mixture was then treated with n-BuLi dropwise and allowed to stir at -78 °C for 20 minutes, followed by dropwise addition of SiCl₄ and additional stirring for 30 minutes. The dry ice-acetone bath was then removed and the solution was allowed to stir at room temperature for an additional hour. The reaction was quenched with hydrochloric acid. After

workup, TLC showed only one spot by UV, until the plate was dyed with PMA and an additional four spots were observed using 1:1 hexanes/ethyl acetate. The crude NMR in CDCl₃ showed expected peaks in the aromatic region, but also many peaks in the alkyl region due to impurities. A silica plug (hexanes) was used to remove some impurities. Several recrystallizations were attempted various ways using chloroform and ethanol. Crystals did form, but every time when trying to collect them they were too small and went through the filter paper. Due to the small amount of oil obtained, it was decided the reaction needed to be performed on a larger scale to make further analysis.

Recently, more 3,6-dihydroxyxanthone has been synthesized and protected with MEM groups. Once purified, we will have enough starting material to try a model reaction using 2-bromotoluene in place of 2-iodotoluene to see whether the Tokyo Green chromophore can be made now that we found improved conditions for the reaction. Then, if successful we can try the synthesis of the array using the tetrakis(4-bromo-2-methylphenyl)silane (Scheme 12). If we can successfully prepare the tetrakis(4-iodo-2-methylphenyl)silane, then we will use it for the final reaction towards the array.



Scheme 12. Proposed model reaction and reaction to target array 1.

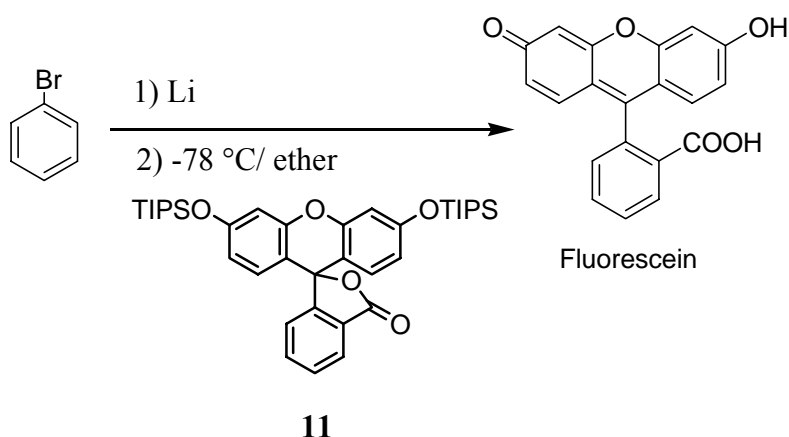
IV. Future Work

After successfully synthesizing our target array **1**, we will characterize the physical, chemical, and optical properties. We will measure the array's absorption and emission spectra, test its water solubility and stability under physiological conditions, and its fluorescence anisotropy. We will examine whether the three-dimensional assembly affects the fluorescence of the component chromophores, comparing it to the chromophore building block alone. In addition, the array's quantum yield and efficiency will be determined. Most importantly, the arrays will be modified with a linker to allow for attaching to a substrate for study, such as a protein. After an appropriate acceptor array has been synthesized, we will be able to perform FRET experiments and analyze the angular dependence of FRET with these arrays.

V. Experimental

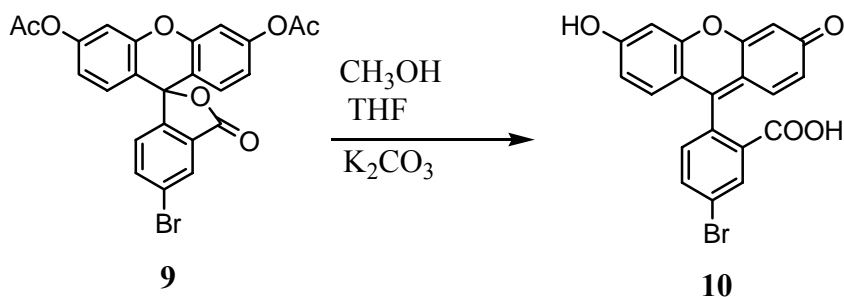
THF and ether were dried and distilled freshly from sodium/benzophenone.

Anhydrous DMF was purchased from ACROS and used directly.



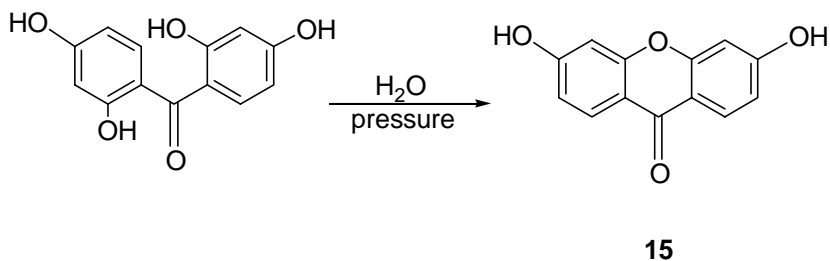
Test of stability of **11** in the presence of PhLi:

Dry ether (2 mL) was added to a flask containing oven-dried pieces of lithium (0.112 g) and stirred under argon. The flask was cooled to -78 °C, then bromobenzene (0.42 mL) and dry ether (1 mL) was added and allowed to stir. To the TIPS-protected fluorescein flask (50 mg), dry ether (2 mL) was added to dissolve it and this solution was added slowly to the flask containing the cooled solution via cannula. When the temperature rose to room temperature it turned dark in color. The TLC (1:1 hexanes/ethyl acetate) showed unreacted bromobenzene and deprotected fluorescein.



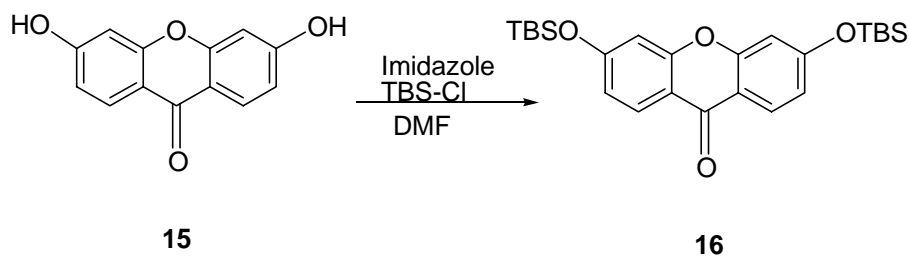
5-Bromofluorescein (**10**) (deprotection of acetal groups):²²

5-Bromofluorescein diacetate (**9**, 450 mg, 0.9 mmol) was dissolved in 30 mL methanol and 15 mL THF, then K_2CO_3 (100 mg, 0.72 mmol) was added. The mixture was stirred at room temperature for 6 h, and then the solvent was removed and 30 mL water was added. The pH was adjusted to 3-4, and a small amount of yellow-green precipitate was formed. The aqueous layer was extracted by ethyl acetate (4×30 mL). The combined organic layers were dried with MgSO_4 and concentrated *in vacuo* to afford a red brown powder (**10**, 379.8 mg, 96.4 %) ^1H NMR (300 MHz, DMSO-d_6) δ 8.15 (d, 1H), 7.85-82 (dd, 1H), 7.19-7.16 (d, 1H), 6.67-6.64 (d, 1H), 6.52-6.44 (m, 4H).³⁸



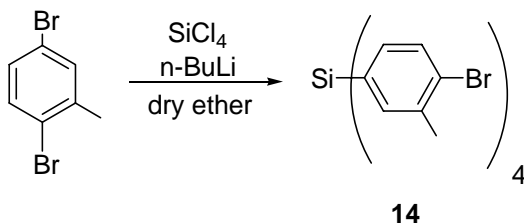
3, 6- Dihydroxyxanthone **15**:

2, 2', 4, 4'- Tetrahydroxybenzophenone (2.51 g) was added to a 50-mL pressure tube containing deionized water (20 mL). The reaction mixture was stirred and heated at 195-200 °C in an oil bath for 6 h, then the solid was filtered off by gravity filtration and washed extensively with hot water (200 mL, 60 °C). The product was heated with water (15 mL) at reflux for 15 min, then cooled to 60 °C, filtered, washed with more hot water and dried in a vacuum oven. Pure compound **15** was obtained as a red-brown powder (586 mg, 23%). Mp > 350 °C. ¹H NMR (400 MHz, DMSO) δ 10.82 (s, 2H), 7.98 (d, 2H, J = 8.6 Hz), 6.85 (m, 4H). IR (KBr): 3384, 3137, 1613, 1456, 1256, 1174, 1117, 848 cm⁻¹.³¹



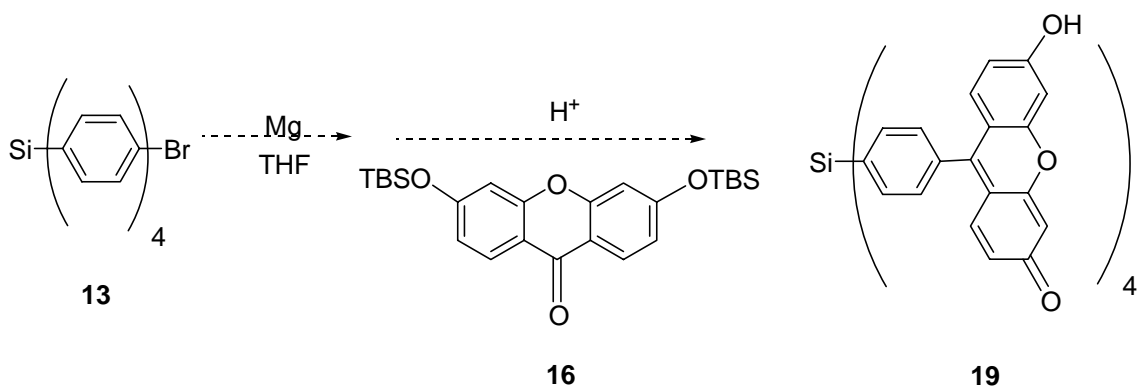
Xanthone bis-TBS ether **16**:

Compound **15** (586.0 mg, 2.57 mmol), imidazole (1.749 g, 25.7 mmol) and TBS-Cl (2.324 g, 15.42 mmol) were dissolved in dry DMF and the solution was allowed to stir overnight under Ar. Then the reaction mixture was extracted with toluene (100 mL), washed extensively with water (2 x 100 mL), and dried with Na₂SO₄. Evaporation *in vacuo* gave an orange solid which was recrystallized from chloroform/ethanol to give shiny white crystals (479.0 mg, 81.7%). Mp 152-154 °C. ¹H-NMR (400 MHz), δ 0.28 (s, 12 H), 1.011 (s, 18 H), 6.83-6.87 (m, 4H), 8.19-8.21 (m, 2H, J = 9.0 Hz).³³ IR (KBr): 3072, 2928, 2856, 1780, 1614, 1444 cm⁻¹.



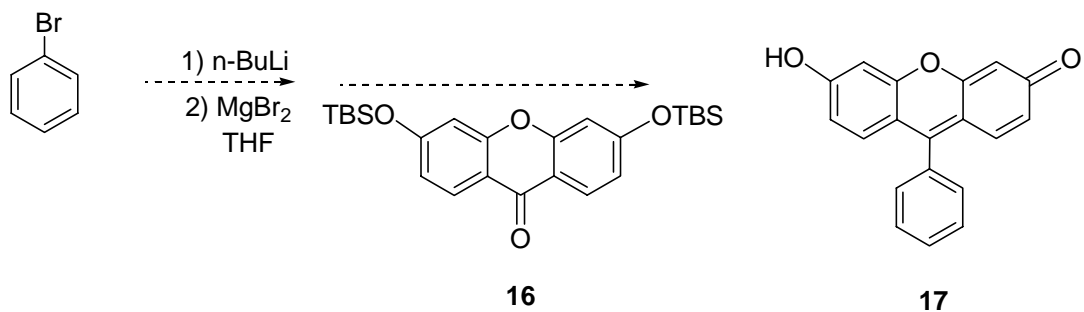
Tetrakis(4-bromo-2-methylphenyl)silane **14**.³²

In a RBF filled with Ar, 2,5-dibromotoluene (1.25 g, 5.0 mmol) and dry ether (10 mL) were cooled to -10 °C. Dropwise, n-butyl lithium (1.6 M in hexanes, 3.13 mL, 5.0 mmol) was added, and the solution was kept at -10 °C for 15 min. SiCl₄ (0.13 mL, 1.25 mmol) was added dropwise, and the mixture was kept at -10 °C for an additional 30 min, allowed to warm up slowly and then kept at 25 °C for 3 h. To quench the reaction, cold HCl (1 M, aq) was added until no more bubbles formed. The mixture was then extracted with ether (3 x 50 mL), washed with water (100 mL) and brine (100 mL) and dried over Na₂SO₄. The residue was recrystallized several times from CHCl₃/ethanol to give a white solid. (84 mg, 10 %). ¹H NMR (400 MHz, CDCl₃) δ 7.55-7.58 (d, 4H, J = 8.0 Hz), 7.32-7.33 (d, 4H, J = 0.8 Hz), 7.15-7.17 (m, 4H), 2.38 (s, 12H), ¹³C NMR (400 MHz, CDCl₃) δ 138.3, 137.7, 135.0, 132.3, 132.2, 127.8, 23.0.³⁸ IR (KBr): 3050, 1780, 1569, 1478, 1377 cm⁻¹.



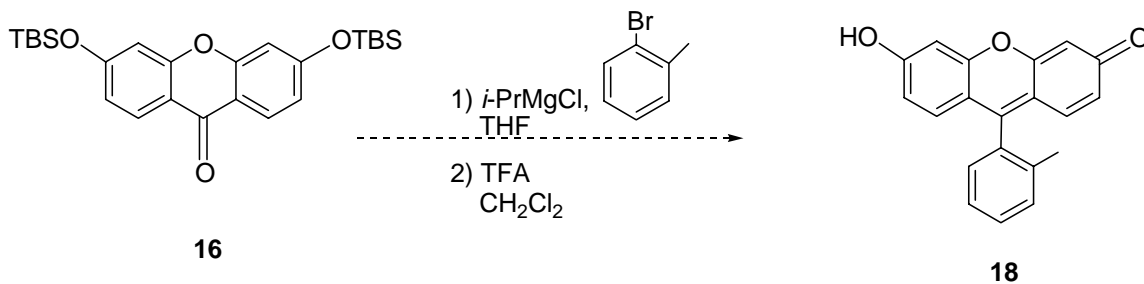
Model Reaction 1:¹⁶

In a RBF, magnesium turnings (23.5 mg, 0.92 mmol) were dried under argon for 3 h. After cooling to room temperature, tetra(bromophenyl)silane **13** (17.5 mg, 0.023 mmol) dissolved in distilled THF (2 mL) was added via cannula. The mixture stirred at 60 °C for 15 min before cooling to room temperature. The solution was then cooled to 0 °C, bis-TBS xanthone **16** (36.6 mg, 0.092 mmol) in THF (2 mL) was added, and the mixture stirred for 15 min. The reaction was quenched with 2M HCl (10 mL) and the resulting crude white precipitate was collected by filtration and washed with THF. ¹H-NMR (400 MHz, CD₃OD) analysis indicated the presence of starting materials **13** and **16**, along with unknown peaks in the alkyl region.



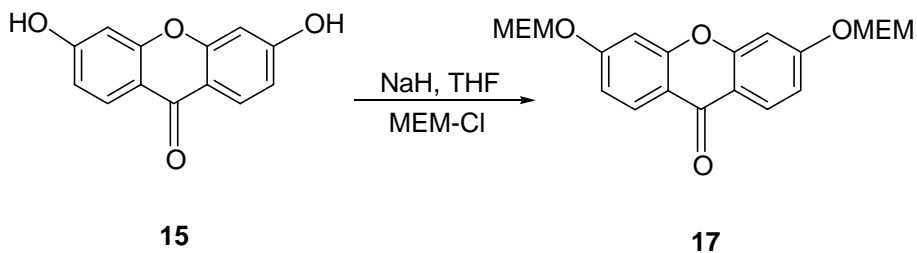
Model Reaction 2:

Bromobenzene (0.12 mL, 1.0 mmol) was stirred under argon with THF (3 mL). The solution was cooled to -78 °C before adding dropwise via syringe, 1.4 M n-BuLi in hexanes (0.75 mL, 1.05 mmol). The mixture was allowed to stir 30 min. By cannula, MgBr₂ (93.89 mg, 0.51 mmol) dissolved in THF (2 mL) was added, and the mixture stirred for 30 min before warming to room temperature. The solution was allowed to stir for an additional 1.5 h at room temperature, then was cooled to 0 °C. Bis-TBS xanthone **16** (433 mg, 1.0 mmol) in THF (3 mL) was added, and the mixture stirred for 4.5 h. The reaction was quenched with 2 M HCl (3 mL), and the solution turned orange. The mixture was extracted with THF (50 mL), washed with brine (50 mL), and dried with magnesium sulfate. After purification by flash column chromatography (10:1 hexanes/ethyl acetate, ethyl acetate, methanol), five fractions were isolated. ¹H-NMR (400 MHz, CDCl₃) analysis indicated one fraction contained starting material **16**, but there was no evidence of bromobenzene or product **17**. Unidentified peaks were observed in the range of 5.0-5.8 ppm and at 9.7 ppm (t).



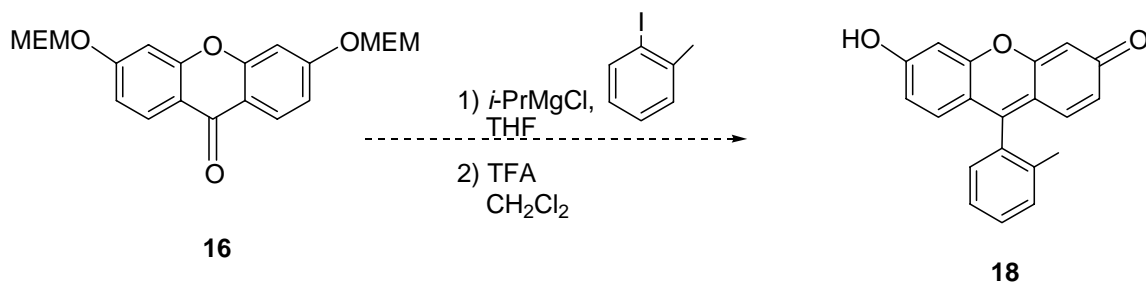
Model reaction 3: Tokyo Green **18**⁷

To an RBF flushed with argon, 2-bromotoluene (0.072 mL, 0.6 mmol), dry THF (2.5 mL), and *i*-PrMgCl (0.3 mL, 0.6 mmol, 2M) were added. The solution was stirred at room temperature for 2 h. Bis-TBS xanthone (**16**, 50 mg, 0.11 mmol) was added and the solution stirred at 22 °C for 19 h. The reaction was quenched with MeOH (2.5 mL) and the solvent was removed *in vacuo*. The resulting residue was redissolved in CH₂Cl₂ (5 mL), treated with TFA (0.25 mL) and stirred an additional 2 h at room temperature. The solvent was removed *in vacuo* to give a yellow oily solid. ¹H NMR (300 MHz, CD₃OD) analysis indicated both starting materials bromotoluene and **16**, as well as unidentified peaks in the 0-1.0 ppm region.



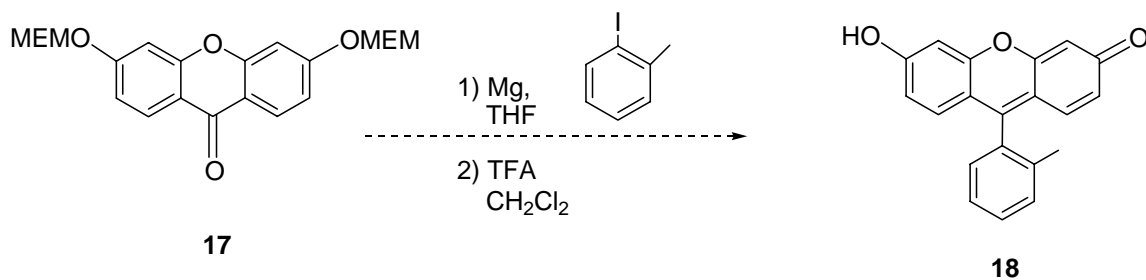
3,6-Bis-(2-methoxy-ethoxymethoxy)-xanthen-9-one **17**:

A solution of 3,6-dihydroxyxanthone (**16**, 100 mg, 0.413 mmol) in dry THF (10 mL) was cooled to 4 °C in an ice bath and NaH (82.6 mg, 2.07 mmol) was added. The solution was allowed to stir for 30 min followed by the addition of 2-methoxyethoxymethyl chloride (MEM-Cl, 0.236 mL, 2.07 mmol) via cannula. The mixture was allowed to warm to room temperature and stirred for 20 h. Saturated NH₄Cl (5 mL) was used to quench the reaction followed by extraction with ethyl acetate (3 x 100 mL). The organic layer was washed with saturated aqueous NaCl and dried with magnesium sulfate. The solvent was removed *in vacuo*. Flash column chromatography (1:1:0.5, hexanes/CH₂Cl₂/ethyl acetate) afforded a white solid that was recrystallized from chloroform and ethanol to give **17** (111.8 mg, 65% yield) as white crystals, mp 107-108 °C (lit. 106-108°C)³⁴. ¹H NMR (300 MHz, CDCl₃) δ 8.2 (d, J = 8.8 Hz, 2H), 7.05 (d, J = 7.8 Hz, 2H), 6.99 (dd, J = 8.4, 5.7, 2H), 5.35 (s, 4H), 3.82 (m, 4H), 3.54 (m, 4H), 3.35 (s, 6H). IR (KBr): 3100, 2903, 1785, 1621, 1442 cm⁻¹.³⁴



Model reaction 4, Trial 1: Tokyo Green 18³⁴

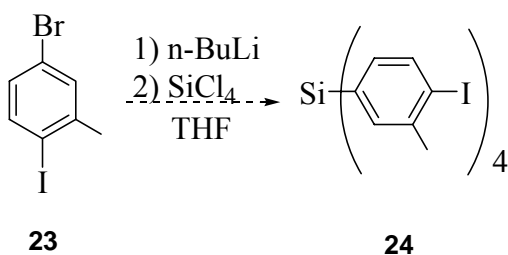
To an RBF flushed with argon, 2-iodotoluene (0.15 mL, 1.19 mmol), dry THF (5 mL), and *i-Pr*MgCl (2 M, 0.6 mL, 1.19 mmol) were added. The solution was stirred at room temperature for 2 h. Bis-MEM xanthone **17** (100 mg, 0.24 mmol) was added and the solution stirred at 22 °C for 18 h. The reaction was quenched with MeOH (5 mL) and the solvent was removed *in vacuo*. The resulting residue was redissolved in CH₂Cl₂ (10 mL), treated with TFA (0.5 mL) and stirred an additional 2 h at room temperature. The solvent was removed *in vacuo* to give a red-orange oily solid. Flash column chromatography (1:20 MeOH/CH₂Cl₂) separated three of the five components seen by TLC. ¹H NMR (300 MHz, CDCl₃) analysis indicated one fraction contained 2-iodotoluene, and another fraction gave a ¹H NMR with aromatic peaks in the range of 6.6 ppm to 8.3 ppm.



Model reaction 5, Trial 1: Tokyo Green 18

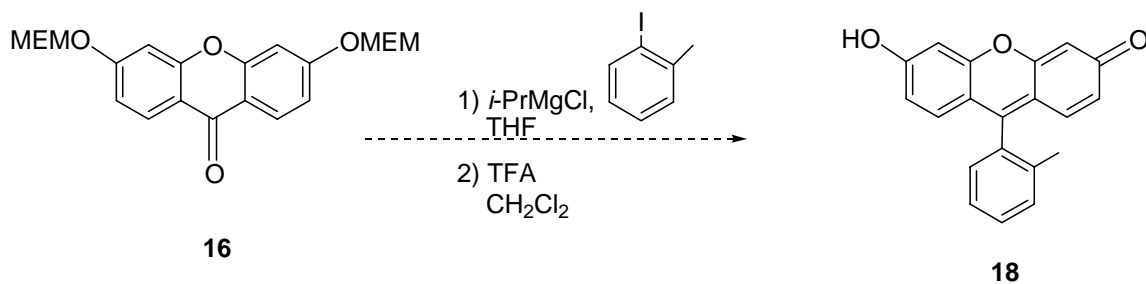
To a flame dried RBF containing dried magnesium turnings (87.13 mg, 3.58 mmol), 2-iodotoluene (0.12 mL, 0.96 mmol) dissolved in dry THF (4 mL) was added and allowed to reflux 2 h. The reaction mixture was cooled to 0 °C, then bis-MEM xanthone (100 mg, 0.24 mmol) dissolved in dry THF (2 mL) was added via cannula. The reaction was allowed to warm to room temperature over 16 h and then quenched with MeOH (10 mL). The solvent was removed *in vacuo* and on the resulting residue column chromatography (1:20 MeOH/CH₂Cl₂) was carried out. ¹H NMR (300 MHz, CDCl₃) analysis indicated the presence of **17**, but there was no 2-iodotoluene observed and two fractions contained aromatic protons. The two fractions were redissolved in CH₂Cl₂ (10 mL), treated with TFA (0.5 mL) and stirred at room temperature for 2 h. The solvent was again removed *in vacuo*. ¹H NMR (300 MHz, CD₃OD) showed that one of the fractions contained new aromatic peaks in the desired range. The fraction was purified by flash column chromatography (1:20 MeOH/CH₂Cl₂). Analysis of the fractions

isolated in the second column (300 MHz, CD₃OD) indicated peaks at 8.0 ppm and 6.8 ppm, but none in the range for the desired product.



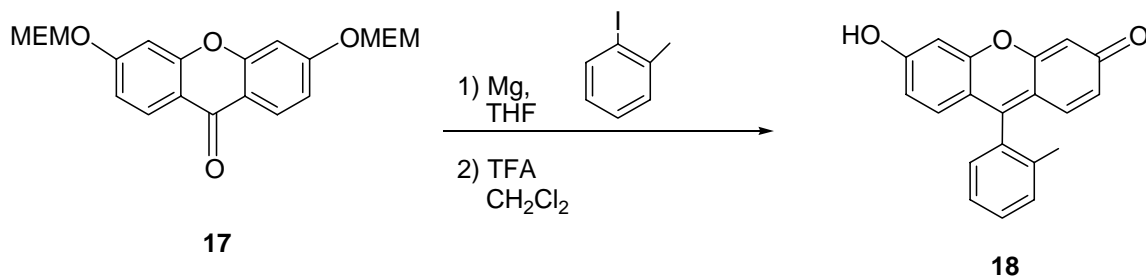
Tetrakis(4-iodo-2-methylphenyl)silane **24**.³²

A solution of 5-bromo-2-iodotoluene (0.48 mL, 3.4 mmol) in THF (20 mL) was allowed to stir at -78 °C under argon. The mixture was treated with n-BuLi (1.3 M in hexanes, 2.62 mL, 3.4 mmol) dropwise. The resulting mixture was kept at -78 °C for 20 min, then SiCl₄ (0.09 mL, 0.85 mmol) was added dropwise. The mixture was stirred at -78 °C for 30 min and then at 25 °C for 1 h. Then 1 M aqueous HCl (10 mL) was added to quench. The organic phase was washed with saturated aqueous Na₂S₂O₃, water, and brine and dried over magnesium sulfate. Recrystallization was attempted using chloroform and ethanol. ¹H NMR (300 MHz, CDCl₃) analysis indicates a mixture of products, with peaks observed in the aromatic range of 6.9-7.7 ppm and unidentified peaks observed in the alkyl region from 0.85 ppm to 2.6 ppm.



Model reaction 4, Trial 2: Tokyo Green 18³⁴

To an RBF flushed with argon, 2-iodotoluene (0.15 mL, 1.19 mmol), dry THF (5 mL), and *i*-PrMgCl (0.6 mL, 1.19 mmol, 2M) were added. The solution was stirred at room temperature for 2 h. Bis-MEM xanthone **17** (100 mg, 0.24 mmol) was added and the solution stirred at 22 °C for 18 h. The reaction was quenched with MeOH (5 mL) and the solvent was removed *in vacuo*. The resulting residue was redissolved in CH₂Cl₂ (10 mL), treated with TFA (0.5 mL) and stirred an additional 2 h at room temperature. The solvent was removed *in vacuo* to give an off-white solid. ¹H NMR (300 MHz, CD₃OD) analysis indicated none of the desired product was present; only unidentified peaks were observed at 7.9 ppm (m) and 6.7-6.9 ppm.



Model reaction 5, Trial 2: Tokyo Green **18**

Magnesium turnings and xanthone **17** were dried in a vacuum oven for 3 d at 80 °C with fresh P₂O₅. To a flame-dried RBF containing dried magnesium turnings (95.84 mg, 3.94 mmol), 2-iodotoluene (0.17 mL, 1.05 mmol) dissolved in dry THF (4 mL) was added and allowed to reflux 2 h. The reaction mixture was cooled to 0 °C, then bis-MEM xanthone (100 mg, 0.26 mmol) dissolved in dry THF (5 mL) was added via a cannula that has been dried in an oven and cooled in a dessicator. The reaction was allowed to warm to room temperature over 16 h and then quenched with MeOH (5 mL) and 2 M HCl (5 mL). The organic phase was extracted with CH₂Cl₂ and dried with magnesium sulfate. The solvent was removed *in vacuo* and the resulting residue was a deep red-orange oil. A plug was used to remove 2-iodotoluene starting material (SiO₂, 1:1 hexanes/ethyl acetate). The solution was treated with TFA (0.5 mL) and stirred at room temperature for 2 h a total of three times. The solvent was again removed *in vacuo* and the resulting red-orange solid was purified by flash column chromatography (1:20 MeOH/CH₂Cl₂) to give Tokyo Green (**18**, 423 mg, 59 %).

Mp > 300 °C. ¹H NMR (300 MHz, CD₃OD) δ 7.48-7.62 (m, 5H), 7.31-7.32 (m, 3H), 7.18- 7.22 (dd, 2H, J = 2.2, 9.2 Hz), 2.05 (s, 3H).³⁴

VI. References

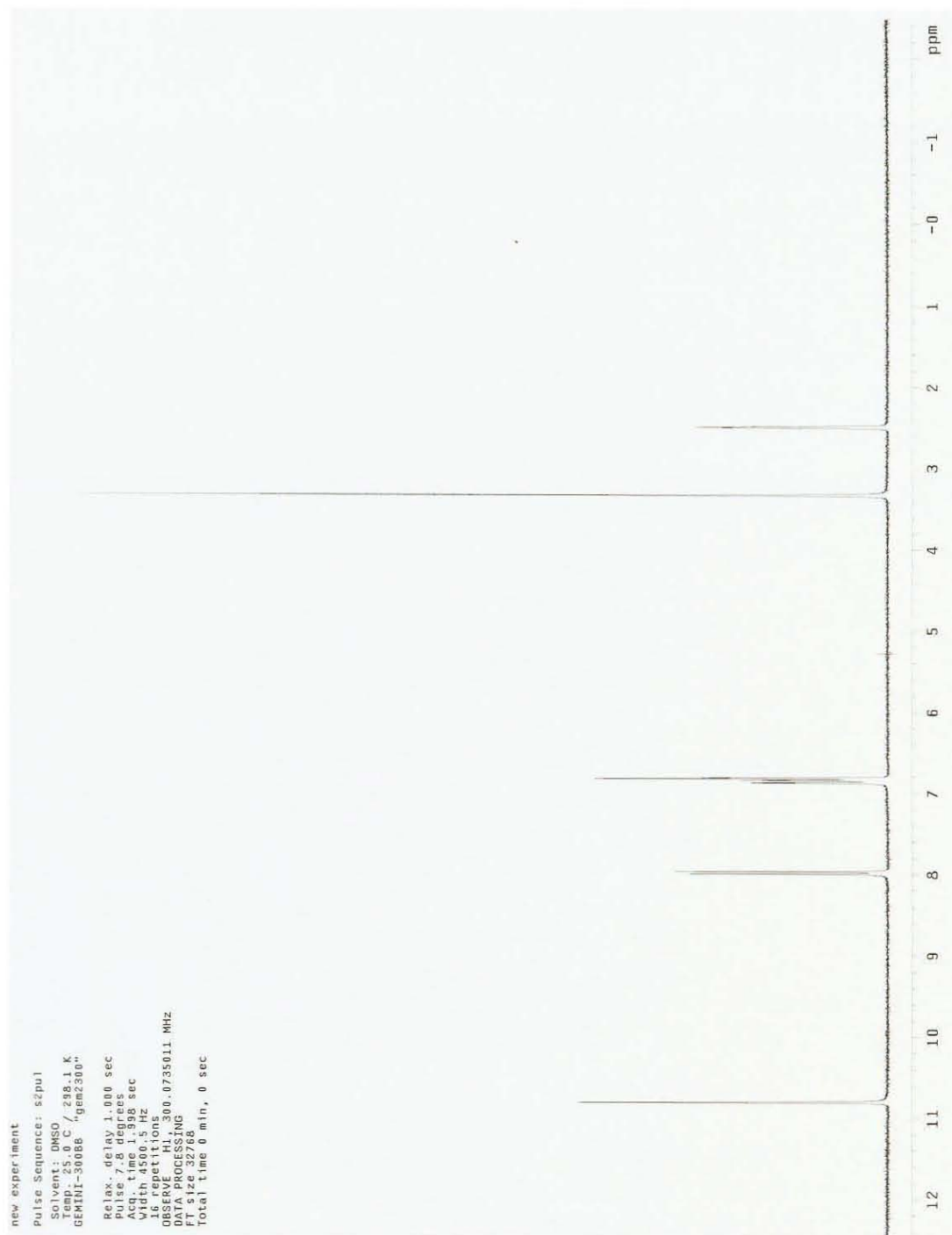
1. Andrews, D. L.; and Demidov, A.A., *Resonance Energy Transfer*, John Wiley and Sons: New York, NY, 1999.
2. van der Meer, B. W.; Coker, G. I.; Chen, S.-Y.S., *Resonance Energy Transfer: Theory and Data*. Wiley-VCH: New York, NY, 1994.
3. Ha, T., Enderle, T., Ogletree, D.F., Chemla, D. S., Selvin, P. R., and Weiss, S., “Probing the interaction between two single molecules: Fluorescence resonance energy transfer between a single donor and a single acceptor”, *Proc. Natl. Acad. Sci. USA*, **1996**, *93* 6264.
4. Schuler, B., Lipman, E. A., and Eaton, W. A., “Probing the free-energy surface for protein folding with single-molecule fluorescence spectroscopy”, *Nature*, **2002**, *419*, 743.
5. Förster, T., “Zwischenmolekulare Energiewanderung und Fluoreszenz”, *Annalen der Physik*, **1948**, *2*, 55; English translation: “Intermolecular Energy Migration and Fluorescence”, *Biolog. Phys.* (Mielczarek, E. V., Greenbaum, E., and Knox, R. S., eds.) **1993**, 148.
6. Giepmans, B. N. G., Adams, S. R., Ellisman, M. H., Tsien, R. Y., “The Fluorescent toolbox for assessing protein location and function”, *Science* **2006**, *312*, 217.
7. Xu, Q.-H., Wang, S.; Korystov, D.; Mikhailovsky, A.; Bazan, G.C.; Moses, D.; Heeger, A.J., “The fluorescence resonance energy transfer (FRET) gate: A time-resolved study”, *Proc. Natl. Acad. Sci. U.S.A.* **2005**, *102*, 530.
8. Jian Yang and Mitchell A. Winnik, “The orientation parameter for energy transfer in restricted geometries including block copolymer interfaces: A Monte Carlo study” *J. Phys. Chem.* **2005**, *109*, 18408.
9. Wu, P.-G., and Brand, L., “Orientation factor in steady-state and time-resolved resonance energy transfer measurements”, *Biochemistry* **1992**, *31*, 7939.

10. Schuler, B.; Lipman, E.A.; Steinbach, P. J.; Kumke, M.; and Eaton, W. A., "Polyproline and the "spectroscopic ruler" revisited with single-molecule fluorescence", *Proc. Natl. Acad. Sci. USA*, **2005**, *102*, 2754.
11. Dale, R. E., and Eisinger, J., "Intramolecular distance determined by energy transfer; Dependence on Orientational Freedom of donor and acceptor", *Biopolymers* **1974**, *13* 1573.
12. Ha, T.; Ting, A.Y.; Liang, J.; Caldwell, B.; Deniz, A. A., Schultz, P. G., Chemla, D. S. and Weiss, S., "Single-molecule fluorescence spectroscopy of enzyme conformational dynamics and cleavage mechanism", *Proc. Natl. Acad. Sci. USA*, **1999**, *96*, 893.
13. Martin, V. V. Alferiev, I. S., Weis, A. L., "Amplified fluorescent molecular probes based on 1,3,5,7-tetrasubstituted adamantane", *Tetrahedron Lett.* **1999**, *40*, 223.
14. Kapanidis, A. N., and Weiss, S., "Fluorescent probes and bioconjugation chemistries for single-molecule fluorescence analysis of biomolecules", *J. Chem. Phys.* **2002**, *117*, 10953.
15. Vamavski, O.P.; Ostrowski, J.C.; Sukhomlinova, L.; Twieg, R.J.; Bazan, G.C.; Goodson, T., "Coherent effects in energy transport in model dendritic structure investigated by ultrafast fluorescence anisotropy spectroscopy", *J. Am. Chem. Soc.* **2002**, *124*, 1736.
16. Urano, Y., Kamiya, M., Kojiro, K., Ueno, T., Hirose, K., and Nagano, T., "Evolution of Fluorescein as a Platform for Finely Tunable Fluorescence Probes", *J. Am. Chem. Soc.* **2005**, *127* 4888.
17. Tanaka, K.; Miura, T.; Umezawa, N.; Urano, Y.; Kikuchi, K.; Higuchi, T.; Nagano, T., "Rational Design of Fluorescein-Based Fluorescence Probes: Mechanism-Based Design of a Maximum Fluorescence Probe for Singlet Oxygen", *J. Am. Chem. Soc.* **2001**, *123* 2530.
18. Miura, T.; Urano, Y.; Tanaka, K.; Nagano, T.; Ohkubo, K.; Fukuzumi, S., "Rational Design Principle for Modulating Fluorescence Properties of Fluorescein-Based Probes by Photoinduced Electron Transfer", *J. Am. Chem. Soc.* **2003**, *125*, 8666.

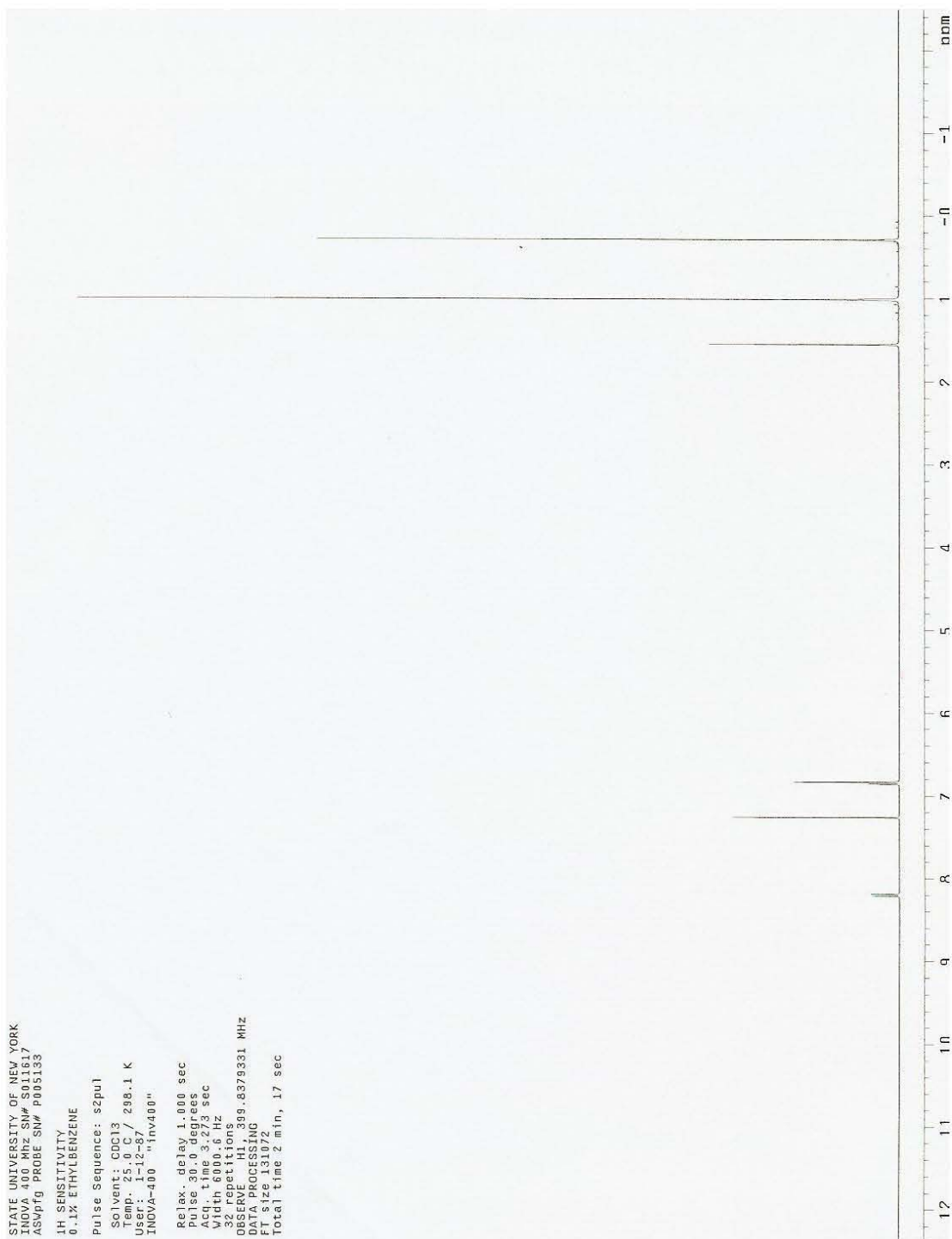
19. Lambert, J.B.; Zhao, Y.; Stern, C. L., "Two-dimensional lattice of superboats composed of silicon-centered tetrahedra", *J. Phys. Org. Chem.* **1997**, 229.
20. Wolf, A.; Roehrscheid, F., "Silicon containing oligocarboxylic anhydrides", *Ger. Offen.* 4229086, Mar. **1994**.
21. Ramette, R. W., and Sandel, E. B., "Rhodamine B Equilibria", *J. Am. Chem. Soc.* **1956**, 78, 4872.
22. Jiao, G.-S.; Han, J.W.; Burgess, K., "Synthesis of Regioisomerically Pure 5- or 6-Halogenated Fluoresceins", *J. Org. Chem.* **2003**, 68, 8264.
23. Greene, T. W.; Wuts, P. G., "Protective Groups in Organic Synthesis", John Wiley and Sons, New York, NY **1999**.
24. Saied, O., Maris, T., Wang, X., Simard, M., and Wuest, J. D., "Submaximal Interpenetration and Bicontinuous Three-Dimensional Channels in Porous Molecular Networks" *J. Am. Chem. Soc.* **2005**, 127, 10008.
25. Bernhard, W., "Etherified Fluorescein Color Formers", US Patent **1991**, 5055595.
26. Mayrargue, J., Essamkaoui, M., and Moskowicz, H., "An Unexpected Difficulty in the Use of MEM as a Protective Group for Phenolic Hydroxyl" *Tetrahedron Lett.* **1989**, 30, 6867.
27. Baptiste, J., Barron, D., et.al., "Effects of Flavanoids on Cell Proliferation and Caspase Activation in a Human Colonic Cell Line HT29: An SAR Study", *J. Med. Chem.* **2005**, 48, 2790.
28. Lippard, S. United States Patent Application, 20020106697.
29. Lundeen, G.W., and Lindqvist L., "Radiationless transitions in Xanthenes", *J. Chem. Phys.* **1966**, 44, 1711.
30. Miura, T.; Urano, Y.; Tanaka, K.; Nagano, T.; Ohkubo, K.; Fukuzumi, S., "Rational Design Principle for Modulating Fluorescence Properties of Fluorescein-Based Probes by Photoinduced Electron Transfer", *J. Am. Chem. Soc.* **2003**, 125, 4666.

31. Shi, J., Zhang, X.P., and Neckers, D.C., "Xanthenes: fluorone derivatives", *J. Org. Chem.* **1992**, *57*, 4418.
32. Fournier, J.-H., Wang, X., and Wuest, J. D., "Derivatives of tetraphenylmethane and tetraphenylsilane: Synthesis of new tetrahedral building blocks for molecular construction", *Can J. Chem.* **2003**, *81*, 376.
33. Minta, A.; Kao, J. P.Y.; Tsein, R.Y.; "Fluorescent Indicators for Cytosolic Calcium Based on Rhodamine and Fluorescein Chromophores", *J. Bio. Chem.* **1989**, *264*, 8171-8178.
34. Peterson, B.; Mottram, L.F.; Boonyarattanakalin, S.; Kovel, R.E., "The Pennsylvania Green Fluorophore: A Hybrid of Oregon Green and Tokyo Green for the Construction of Hydrophobic and pH-Insensitive Molecular Probes", *Org. Lett.* **2006**, *8*, 581.
35. Herman, B.; Centonze Frohlich, V.E.; Lakowicz, J.R.; Fellers, T.J.; Davidson, M.W., "Applications in Confocal Microscopy: Fluorescence Resonance Energy Transfer (FRET) Microscopy", Olympus Confocal Microscopes Resource Center, Oct. 14, 2006.
<<http://www.olympusfluoview.com/applications/fretintro.html>>.
36. dos Remedios, C.G.; Moens, P.D.J., "Fluorescence energy transfer. Spectroscopy is a reliable "ruler" for measuring structural changes in proteins", *J. Struc. Bio.* **1995**, *115*, 175.
37. Wu, P.-G. and Brand, L., "Resonance energy transfer: methods and applications", *Anal Biochem*, **1994**, *218*, 1.
38. Zhou, Lu. "Synthesis of Different Tethered Compounds for Cylindrically Conjugated Organic Belts and Synthesis of Three-Dimensional Assemblies of Chromophores for FRET Studies." PhD Dissertation, SUNY Stony Brook, Chemistry Dept., 2006.
39. Herman, B.; Centonze Frohlich, V.E.; Lakowicz, J.R.; Fellers, T.J.; Davidson, M.W., "Fluorophores for Confocal Microscopy", Olympus Confocal Microscopes Resource Center, July 13, 2007.
<<http://www.olympusfluoview.com/applications/fretintro.html>>.

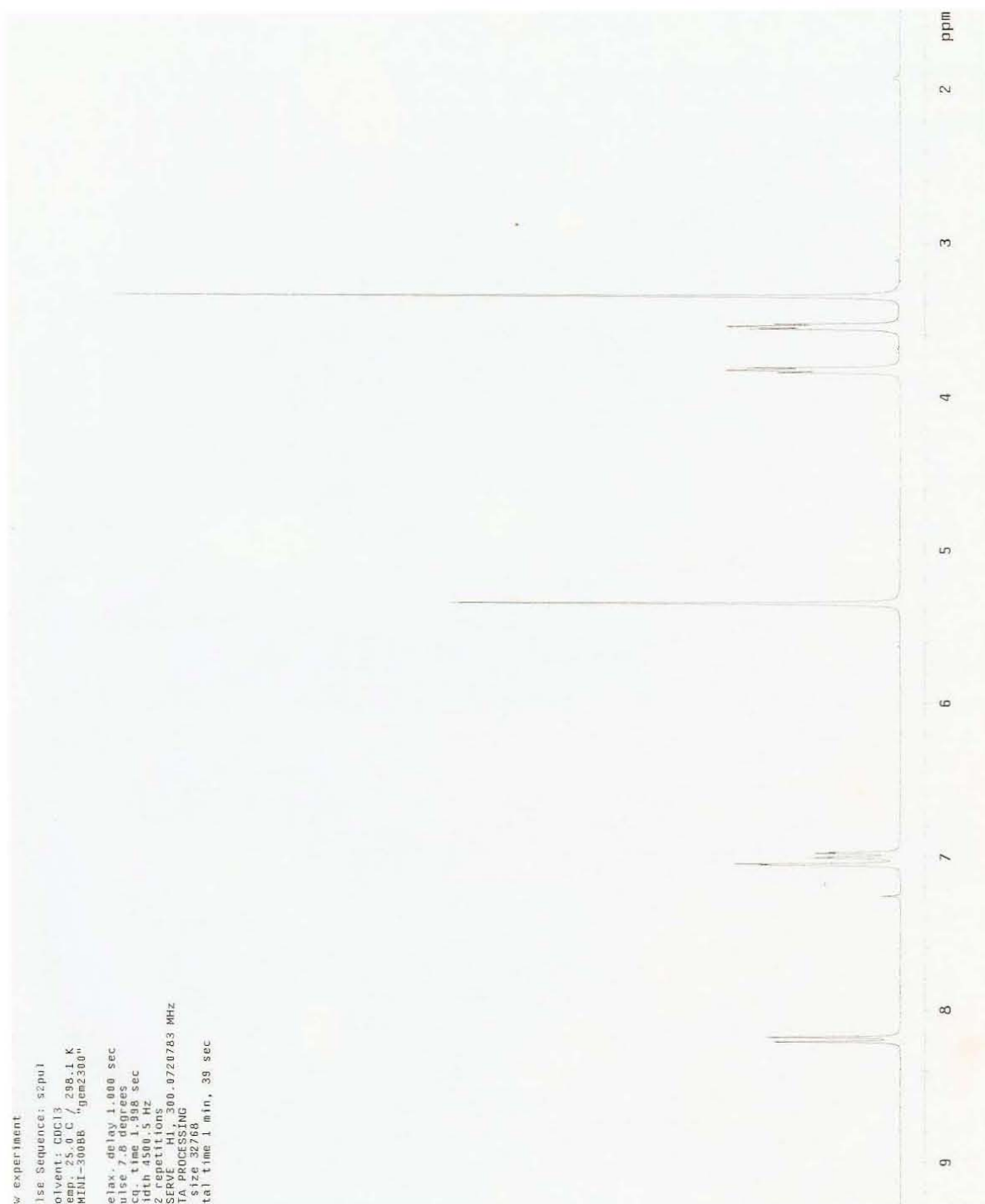
VII. Appendix



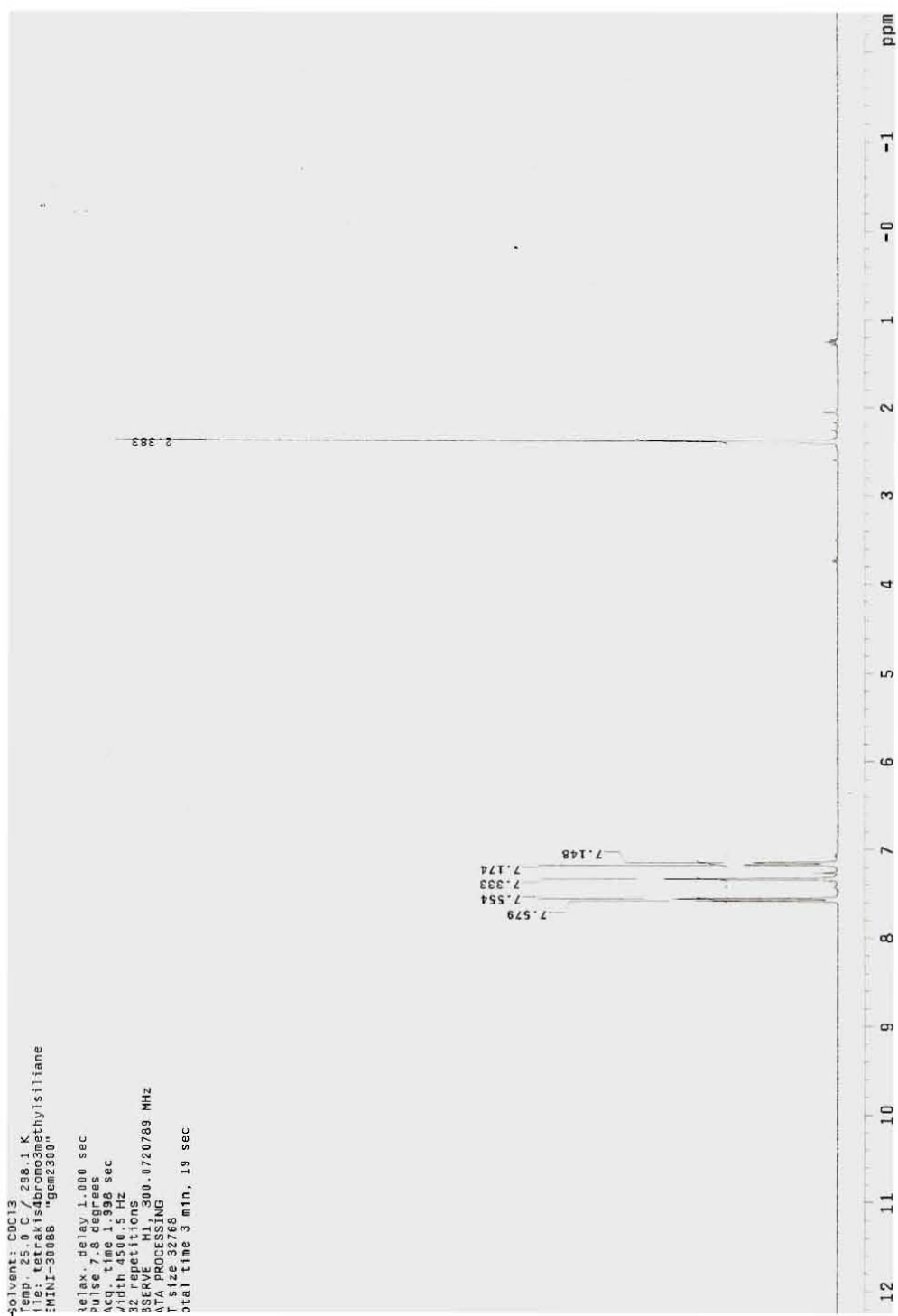
^1H NMR (300 MHz, DMSO): 3, 6-Dihydroxyxanthone **15**



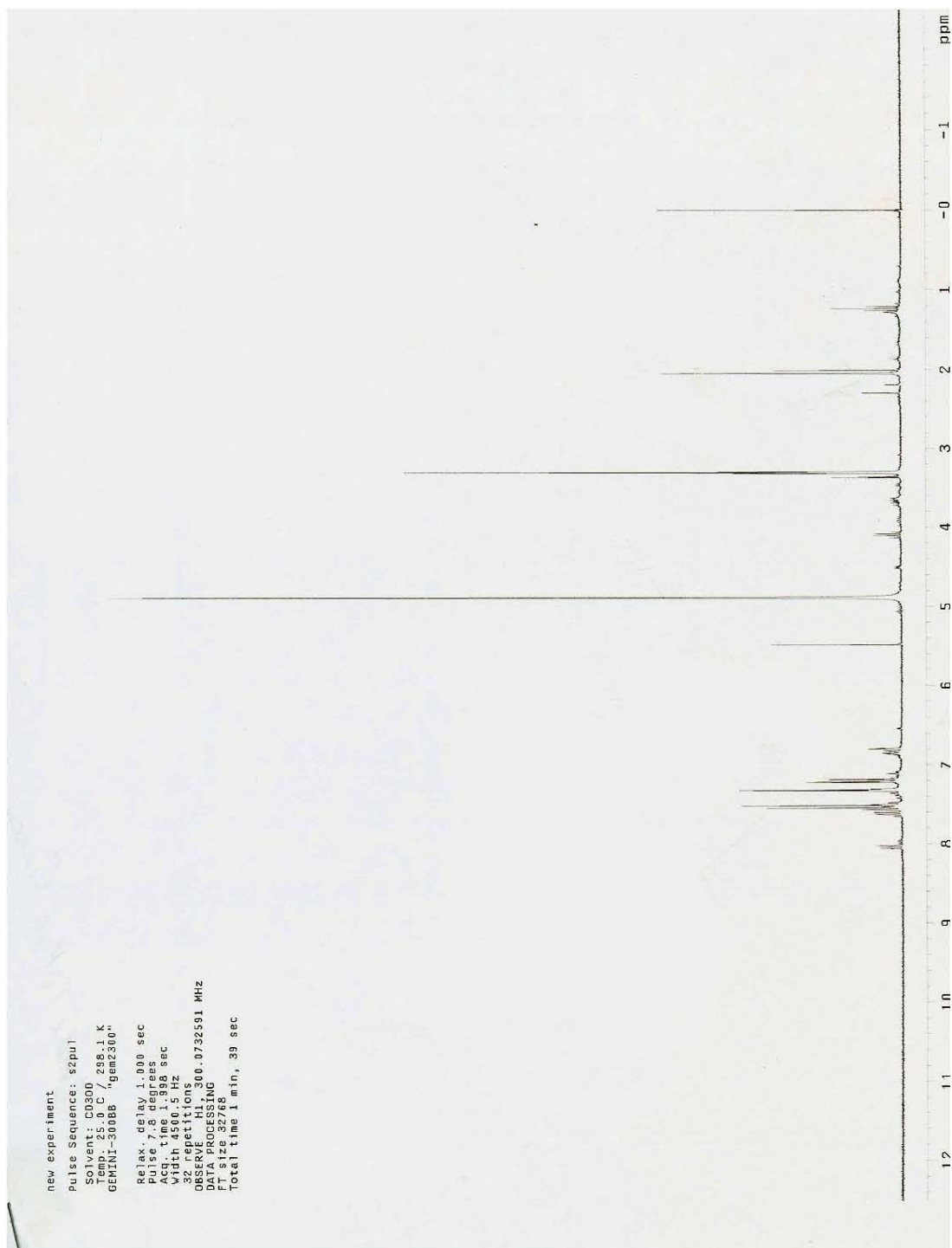
¹H NMR (400 MHz, CDCl₃): Xanthone bis-TBS ether **16**



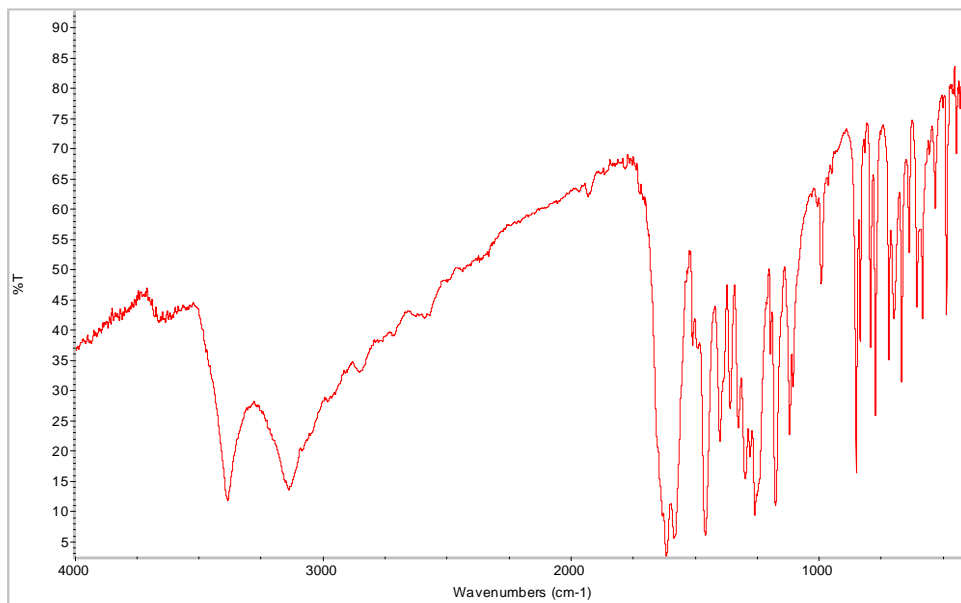
¹H NMR (300 MHz, CDCl₃): 3,6-Bis-(2-methoxy-ethoxymethoxy)-xanthen-9-one



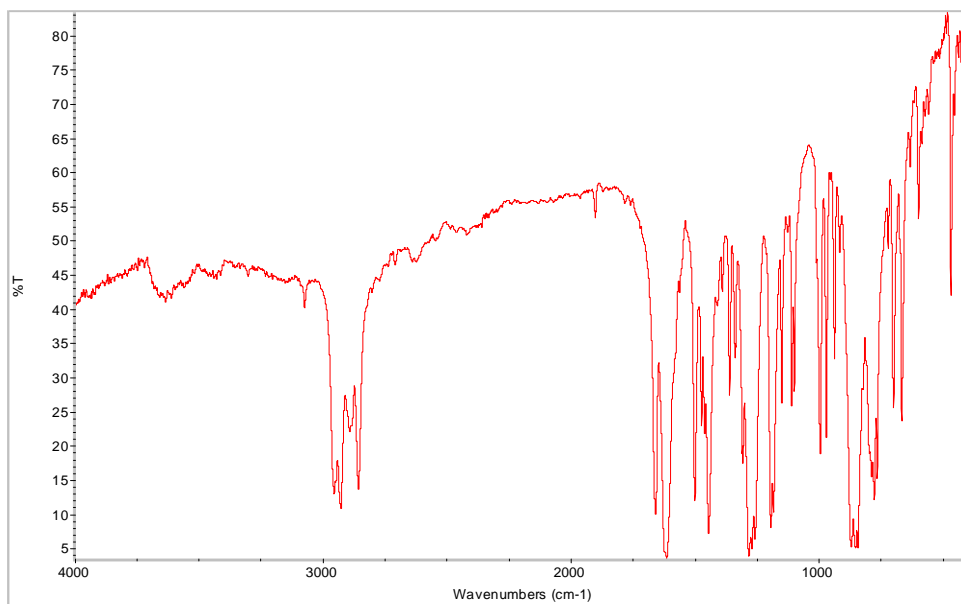
¹H NMR (300 MHz, CDCl₃): Tetrakis(4-bromo-2-methylphenyl)silane **14**



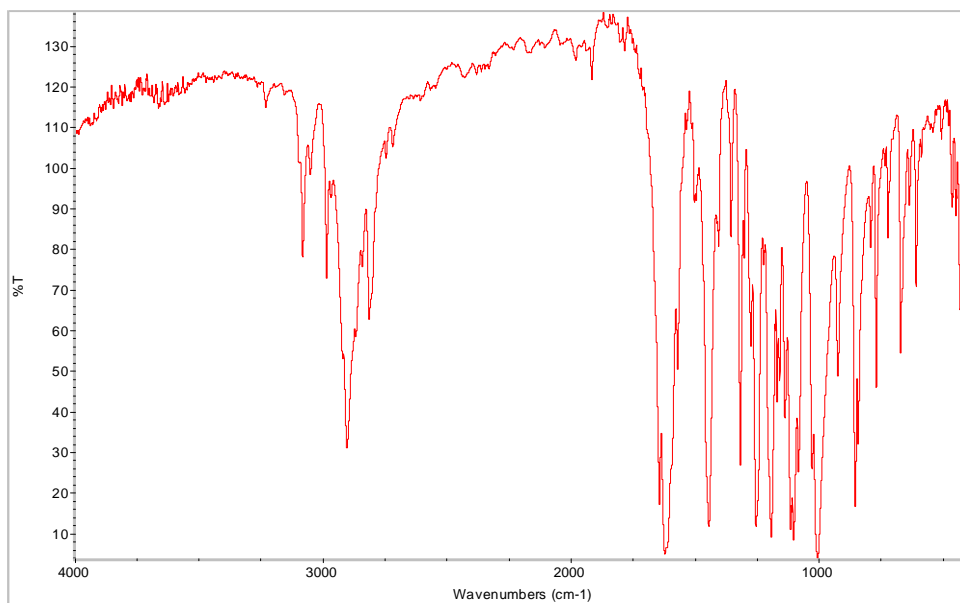
¹H NMR (300 MHz, CD₃OD): crude Tokyo Green **18**



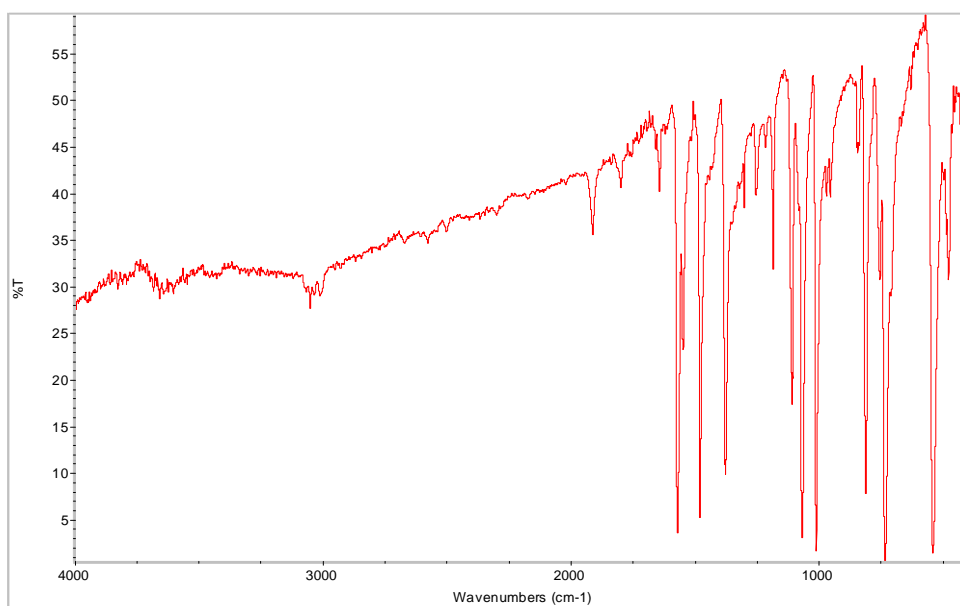
IR (KBr): 3,6- Dihydroxyxanthone **15**



IR (KBr): Xanthone bis-TBS ether **16**



IR (KBr): 3,6-Bis-(2-methoxy-ethoxymethoxy)-xanthen-9-one **17**



IR (KBr): Tetrakis(4-bromo-2-methylphenyl)silane **1**